2012

IMPACT OF 2000-2050 CLIMATE CHANGE ON GLOBAL ATMOSPHERIC TRANSPORT AND DEPOSITION OF MERCURY

Wenchao Chen
Michigan Technological University

IMPACT OF 2000-2050 CLIMATE CHANGE ON GLOBAL ATMOSPHERIC TRANSPORT AND DEPOSITION OF MERCURY

By

Wenchao Chen

A REPORT

Submitted in partial fulfillment of the requirements for the degree of

MASTER OF SCIENCE

In Environmental Engineering

MICHIGAN TECHNOLOGICAL UNIVERSITY

2012

This report has been approved in partial fulfillment of the requirements for the Degree of MASTER OF SCIENCE in Environmental Engineering.

Department of Civil and Environmental Engineering

Report Advisor: Shiliang Wu

Committee Member: Louisa Kramer

Committee Member: Simon Carn

Department Chair: David Hand

Table of Contents

List of Figures

Abstract

Since it is very toxic and accumulates in organisms, particularly in fish, mercury is a very important pollutant and one of the most studies. And this concern over the toxicity and human health risks of mercury has prompted efforts to regulate anthropogenic emissions. As mercury pollution problem is getting increasingly serious, we are curious about how serious this problem will be in the future. What is more, how the climate change in the future will affect the mercury concentration in the atmosphere. So we investigate the impact of climate change on mercury concentration in the atmosphere. We focus on the comparison between the mercury data for year 2000 and for year 2050. The GEOS-Chem

model shows that the mercury concentrations for all tracers (1 to 3), elemental mercury (Hg(0)), divalent mercury (Hg(II)) and primary particulate mercury (Hg(P)) have differences between 2000 and 2050 in most regions over the world. From the model results, we can see the climate change from 2000 to 2050 would decrease Hg(0) surface concentration in most of the world. The driving factors of Hg(0) surface concentration changes are natural emissions(ocean and vegetation) and the transformation reactions between Hg(0) and Hg(II). The climate change from 2000 to 2050 would increase Hg(II) surface concentration in most of mid-latitude continental parts of the world while decreasing Hg(II) surface concentration in most of high-latitude part of the world. The driving factors of Hg(II) surface concentration changes is deposition amount change (majorly wet deposition) from 2000 to 2050 and the transformation reactions between Hg(0) and Hg(II). Climate change would increase Hg(P) concentration in most of mid-latitude area of the world and meanwhile decrease Hg(P) concentration in most of high-latitude regions of the world. For the Hg(P) concentration changes, the major driving factor is the deposition amount change (mainly wet deposition) from 2000 to 2050.

1. Introduction

Mercury is a heavy and silvery-white metal which is very toxic. The chemical symbol of mercury is “Hg” with the atomic number 80. Mercury is the only known metal which is liquid at standard conditions for temperature and pressure. Also, mercury has one of the broadest ranges of its liquid state of any metal with a freezing point of -38.83 degrees C and boiling point of 356.73 degrees C. The density of mercury is 13.534 grams per cubic meter under liquid phase at standard conditions for temperature and pressure. There are different forms of mercury in the atmosphere: elemental mercury (Hg(0)), divalent

mercury (Hg(II)) and primary particulate mercury (Hg(P)). Elemental mercury (Hg(0)) is the major form of mercury in the atmosphere which accounts for about 95% of the total mercury. It has very little solubility in water and can be slowly oxidized to the mercuric state which is divalent mercury (Hg(II)) form. Divalent mercury (Hg(II)) is the second abundant form of mercury in the atmosphere and highly soluble in water with an relative low Henry's law constant (much lower than elemental mercury (Hg(0))). It can partition between gas and particulate phase. Primary particulate mercury (Hg(P)) is not pure particles of mercury but mercury compounds associated with atmospheric particulate. The exact species of primary particulate mercury (Hg(P)) are largely unknown. It only accounts for a few percent of total mercury (Hg) in atmosphere which is only a very small portion of mercury in the air and is chemically inert.

Elemental mercury (Hg(0)) is relatively inert and the atmospheric residence time is about one year. Due to the long life time in the atmosphere, mercury is efficiently transported around the globe (Selin et al. 2007), making mercury pollution an environmental problem at the global scale. Global mercury emissions have increased substantially at least during the past 100 to 150 years (Martinez-Cortizas, A. et al. 1999). Coal combustion, which is the major anthropogenic emission source of mercury, is getting larger year by year (3.3 billion tons produced in year 1990, 4.2 billion tons produced in year 2000 and 5.1 billion tons in year 2010). The mercury pollution can impact the health of people, fish, and wildlife due to its toxicity. Mercury can accumulate in organisms, particularly in fish. The health risks associated with mercury pollution are so strong that many agencies or governments around the world have issued fish consumption advisories (see EPA website for USA details: http://www.usgs.gov/themes/factsheet/146-00/fig4b.gif).

About one third of the total mercury emissions are from anthropogenic sources while the other two thirds are from natural sources which include the re-emissions of those anthropogenic mercury deposited to the Earth surface (Selin et al. 2007). The anthropogenic emissions come from coal fired power plants, metal smelting and waste incineration. Among these anthropogenic sources of mercury, the major form is gaseous elemental mercury which accounts for about 53% of the total emissions and there is 37% gaseous divalent mercury. The particle-associated mercury is only about 10% (Jozef M.Pacyna et al. 2008). The natural sources of mercury include emissions from oceans, soil, and terrestrial vegetation, biomass burning (Selin et al. 2007).

Since it is very toxic and accumulates in organisms, particularly in fish, mercury is a very important pollutant and one of the most studies. And this concern over the toxicity and human health risks of mercury has prompted efforts to regulate anthropogenic emissions. Although local decreases have been seen in some locations (mainly because of the reduction of emissions of regional sources), in general, mercury (Hg) burdens have not declined. Global mercury emissions today range from 4,400 to 7,500 tons per year, according to the Environmental Protection Agency (EPA), and this number is still increasing year by year. As mercury pollution problem is getting increasingly serious, we are curious about how serious this problem will be in the future. What is more, how the climate change in the future will affect the mercury concentration in the atmosphere. So we investigate the impact of climate change on mercury concentration in the atmosphere. We focus on the comparison between the mercury data for year 2000 and for year 2050. Through this comparison, we try to get our conclusion about how climate changes from 2000 to 2050 impact the mercury concentration in the atmosphere. The GEOS-Chem

model shows that the mercury concentrations for all tracers (1 to 3), elemental mercury (Hg(0)), divalent mercury (Hg(II)) and primary particulate mercury (Hg(P)) have differences between 2000 and 2050 in most regions over the world. The main reason of the differences (increases or decreases) is the climate changes between year 2000 and year 2050.

2. Model description

2.1. The GEOS-Chem/GCAP model

GEOS-Chem model is a global 3-D chemical transport model (CTM) for atmospheric composition driven by meteorological fields from the Goddard Earth Observing System (GEOS) of the NASA Global Modeling and Assimilation Office (http://acmg.seas.harvard.edu/geos/). It is used to simulate the emissions, transport, chemical evolution and deposition of a wide range of chemical species in the atmosphere. GEOS-Chem can resolve more than 80 chemical species and 300 reactions. The model is usually initialized with a "restart" file containing concentrations for each species in each grid box. To allow the model to reach chemical equilibrium, a "spin-up" period of typically 6 to 12 months is used for all model runs. We simulated mercury (Hg) emissions, chemistry, and atmospheric deposition using the GEOS-Chem model, described in detail by (Selin et al. 2007, 2008), with updates described by the published paper (Selin and Jacob.2008). The GEOS-Chem simulation has been extensively evaluated against atmospheric concentration and deposition measurements and matches seasonal and spatial trends (Selin et al. 2007, 2008). For the simulations in this paper, the tracers we used are tracers 1-3 (three species of mercury in the atmosphere): elemental

mercury (Hg(0)), divalent mercury (Hg(II)), and primary particulate mercury (Hg(P)). For this study to predict atmospheric mercury concentrations, the model uses simulated meteorological fields from the NASA/GISS Model 3 data as input, including winds, mixed layer depths, temperature, precipitation, and convective mass fluxes.

GCAP is a special version of GEOS-Chem model which stands for 'Global Change and Air Pollution'. It is used to simulate and detect the atmospheric chemicals concentrations in the future. For example, in this paper, we take advantage of GCAP to simulate the mercury concentration in 2049-2051 years so as to make the comparison of mercury concentration between 2000 and 2050 in the atmosphere. We compile the GCAP model by the GEOS-Chem model version 8-03-01**.** Our simulation is conducted for two 3-year periods (1999-2001 and 2049-2051) by GCAP, with the first 3 years (1999-2001) used to get the 3-year average values of Hg(0), Hg(II) and Hg(P), respectively in the year 2000 and the last 3 years (2049-2051) used for getting the 3-year average value of Hg(0), Hg(II) and Hg(P), respectively in the year 2050. It uses simulated meteorological fields from the NASA/GISS Model 3 data as input, including winds, mixed layer depths, temperature, precipitation, and convective mass fluxes. This GCAP meteorological field used by GEOS-Chem is containing A3 fields which are 3-hour time averages, centered on 01:30 04:30 07:30 ... 22:30 GMT, A6 fields which are 6-hour time averages, centered on 00:00 06:00 12:00 18:00 GMT, I6 fields which are 6-hour instantaneous fields, centered on 00:00 06:00 12:00 18:00 GMT and Constant fields which are time-invariant. We focus most of our analyses on the comparison between the mercury data for year 2000 and for year 2050. By the comparison, we try to get our conclusion about how the climate changes from 2000 to 2050 impact the mercury concentration in the atmosphere.

2.2. Model Evaluation

Before using the simulation data which is from the model, we have to do the model data verification. Model data verification is basically the comparison between the data results of the compiled model and the observational data in order to see if there is a big "gap" between them. Since in the model we simulated three different tracers: elemental mercury (Hg(0)), divalent mercury (Hg(II)) and primary particulate mercury (Hg(P)), the observational data we need is also for these three tracers.

The model version we use for the simulation is GCAP which stands for 'Global Change and Air Pollution'. GCAP is used to simulate both present-day and future air quality. So before using the future simulation data results of the GCAP model, we have to make sure the present-day data results match up the observational data or some published data results. So, in the first step of the model data verification, we make the comparison between the GCAP present-day data result for elemental mercury (Hg(0)) in year 2000 (Figure.1) and the published (Lyatt Jaegle.2010) results plotting for annual mean distribution of surface concentration of elemental mercury (Hg(0)) in year 2008 (Figure.2). After compiling all the GCAP simulation components, we make a one year run from Jan.1st, 2000 to Jan.1st, 2001 for elemental mercury (Hg(0)) and make the annual mean surface concentration plot for the whole year 2000 data of elemental mercury (Hg(0)) as shown in Figure.1. The comparable plotting result from a published paper (Lyatt Jaegle.2010) is also the annual mean surface plot for elemental mercury (Hg(0)) but for the year 2008 as shown in Figure.2.

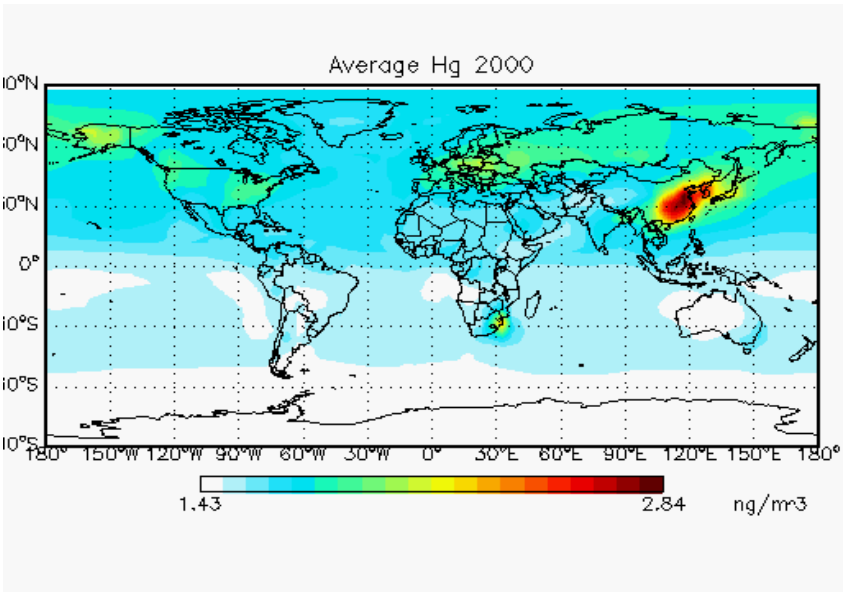

Figure.1. , Annual mean surface concentration plot for year 2000 data of elemental mercury (Hg(0))

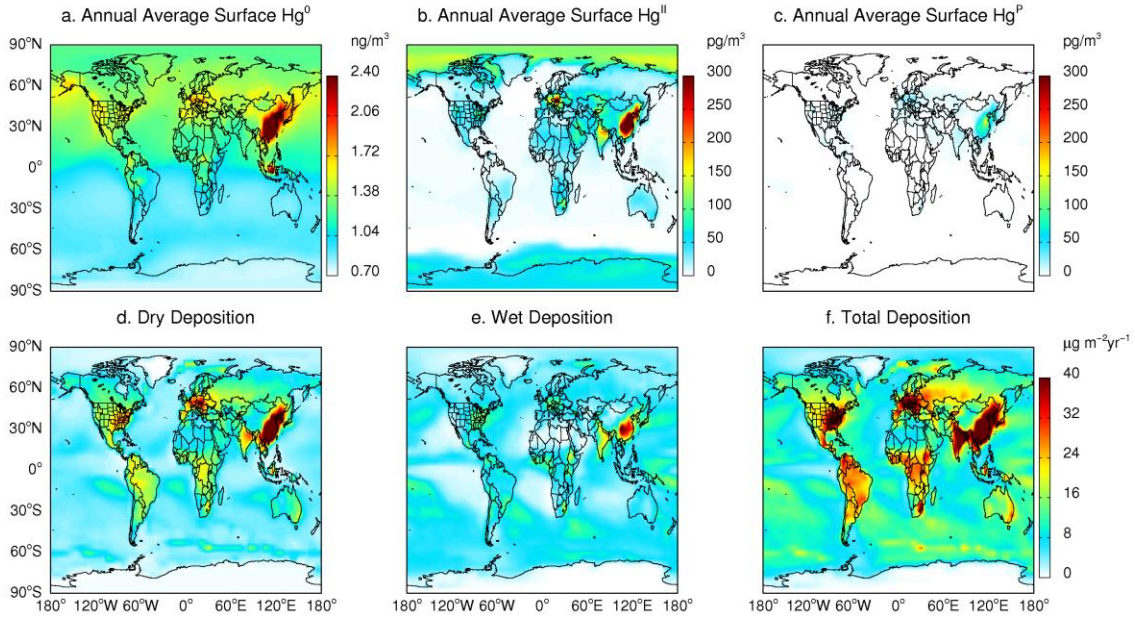

Figure.2. , The published annual mean surface concentration plot of elemental mercury (Hg(0)) for the year 2008 (a) Elemental mercury (Hg(0)), b) Divalent mercury (Hg(II)) and c) Primary particulate mercury (Hg(P)) for 2008. The bottom three figures show the annual mean distribution of deposition fluxes: d) Dry deposition, e) Wet deposition and f) Total deposition (Lyatt Jaegle.2010))

As we can get from the comparison between Figure.1 and Figure.2, the annual mean distribution of surface concentration of elemental mercury (Hg(0)) in both plots are in a very similar shape. The high concentration areas (red) and low concentration areas (white or blue) in both plots are in the same positions, especially the peak values (2.84 and 2.40 ng/m^3). Since the annual mean value of elemental mercury (Hg(0)) in the air for a same place should not vary too much from year to year, this comparison between Figure.1 and Figure.2 can prove that the result of the one year run from Jan.1st, 2000 to Jan.1st, 2001 for elemental mercury (Hg(0)) makes sense. So we know the model works normally for present-day simulation for elemental mercury (Hg(0)).

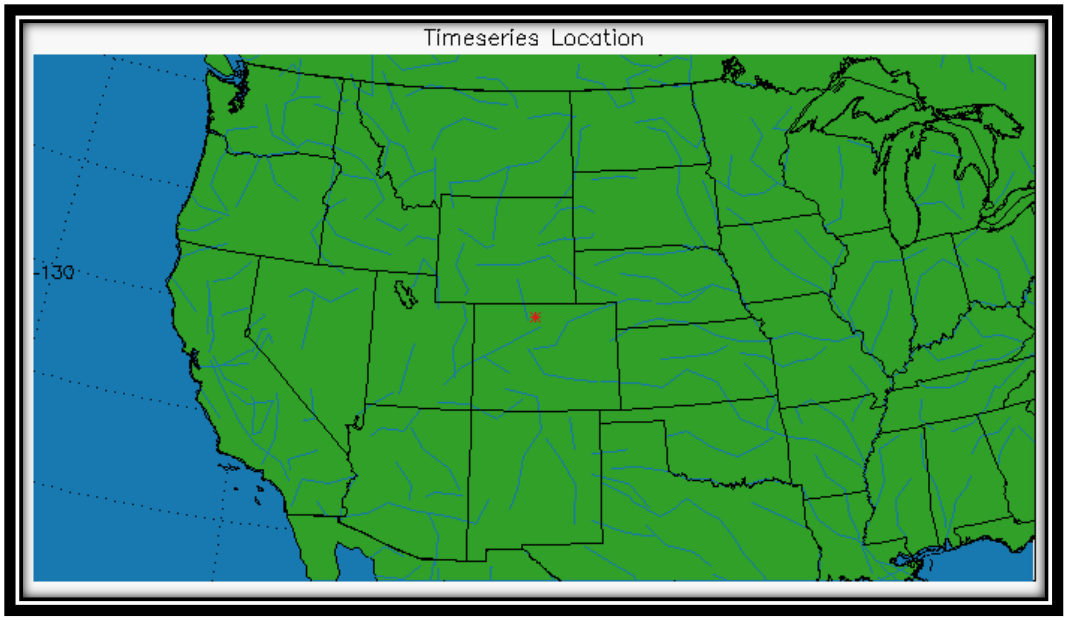

Figure.3, the observation data we use is from the Storm Peak Laboratory (SPL) in Colorado State

For the second step of the model data verification, we plan to use some available observation data to verify the model simulation result of elemental mercury (Hg(0)), divalent mercury (Hg(II)) and primary particulate mercury (Hg(P)). The observation data we use is from the Storm Peak Laboratory (SPL) in Colorado State. SPL is a permanent

mountain-top facility which was constructed during the summer of 1995 in the Rocky Mountains of northwestern Colorado (3220m M.S.L.; 40.455 deg N, -106.744 deg W) as showing in Figure.3. The mission of Storm Peak Laboratory (SPL) is to integrate research and education by advancing discovery and understanding within the field of aerosol and cloud interactions. The mercury observation data from SPL is for all three different tracers: elemental mercury (Hg(0)), divalent mercury (Hg(II)) and primary particulate mercury (Hg(P)) in May and June of 2000. In order to compare with these observation data from SPL, we simulated these three tracers also for May and June in both 1999 and 2000. The data we get from the model is time series data which is 3-hour average value (8 values per day). By using these direct simulation results, 3-hour average values, we get the daily average value by averaging the 8 numbers for each day. So we have 31 values in May dataset and 30 in June dataset meanwhile. The observation data from SPL is 2-hour average value (12 values per day). We also make the daily average value by averaging the 12 numbers for each day. So as same as the model results, we have 31 values in May dataset and 30 in June dataset. The statistics method we use to compare the model dataset and the observation dataset is a “box-plot” as shown in Figure.4 to 6. In the box-plot, the solid line shows the range of the dataset (maximum value in the upper, minimum value in the lower) meanwhile the blue point is the median of the dataset with green shows the mean value. As we can see from Figure 4 to 6, the elemental mercury (Hg(0)) and primary particulate mercury (Hg(P)) between model results and lab results agree reasonably well for both the median and mean values, also for the data range. However, there is a big difference gap of divalent mercury (Hg(II))

between the GCAP model results and the observation results as the box- plot in Figure.5 shows.

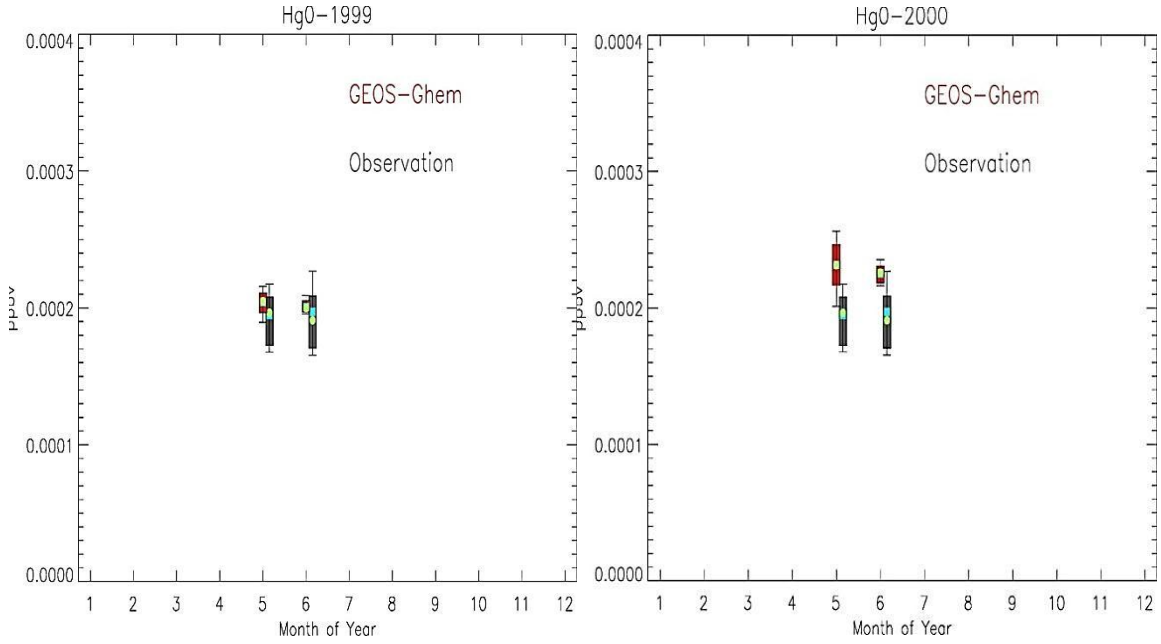

Figure.4, Comparison between model simulation data for elemental mercury (Hg(0)) of May and June in 1999 (left) and 2000 (right) and SPL observation data for elemental mercury (Hg(0)) of May and June in 2000

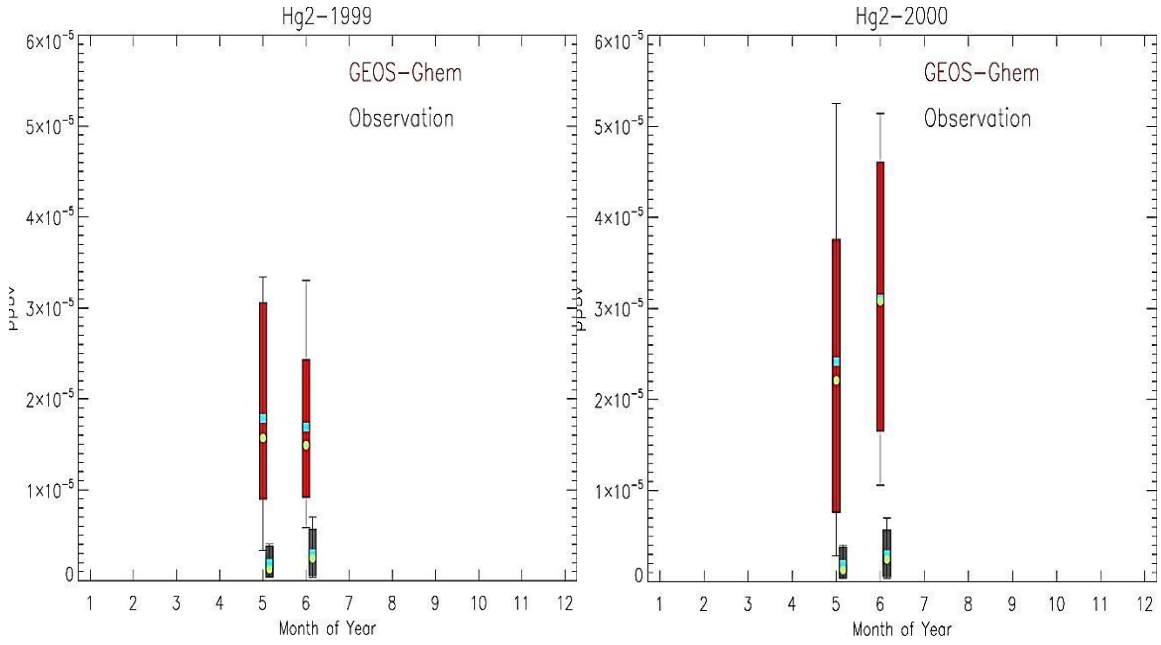

Figure.5, Comparison between model simulation data for divalent mercury (Hg(II)) of May and June in 1999 (left) and 2000 (right) and SPL observation data for divalent mercury (Hg(II)) of May and June in 2000

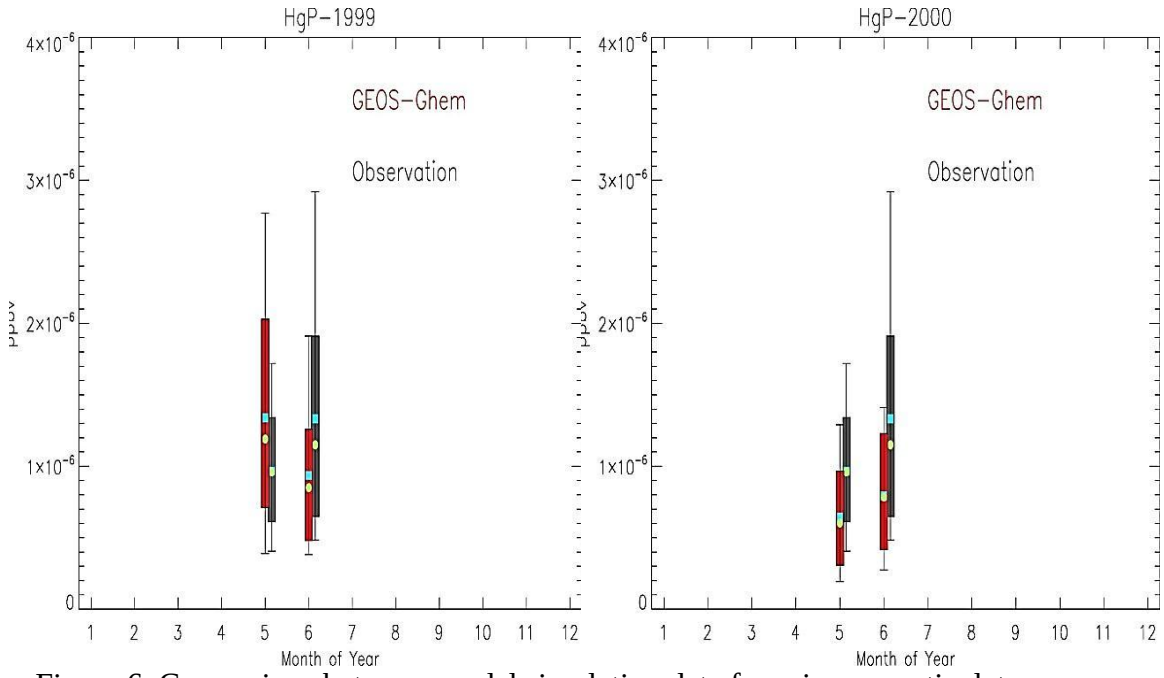

Figure.6, Comparison between model simulation data for primary particulate mercury (Hg(P)) of May and June in 1999 (left) and 2000 (right) and SPL observation data for primary particulate mercury (Hg(P)) of May and June in 2000

So, we use the GEOS-4 model to double-check the GCAP model results of divalent mercury (Hg(II)) by running May and June in 2004 as showing in Figure.7 to 8. From this box-plotting comparison between GEOS-4 result and observation result in Figure.7 to 8, we can see it is very similar with GCAP result. There is still a big gap for divalent mercury (Hg(II)) but good matching up for the elemental mercury (Hg(0)) and primary particulate mercury (Hg(P)). So we get the conclusion that there is no specific mistake on GCAP model running but the common difference between the divalent mercury (Hg(II)) observation data and its model data result.

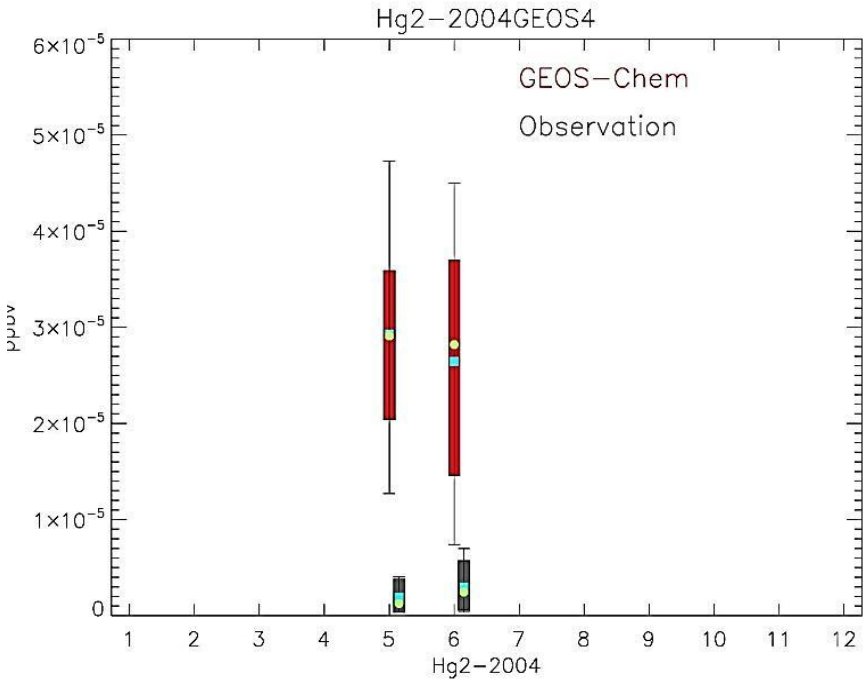

Figure.7, Comparison between GEOS-4 model simulation data for divalent mercury (Hg(II)) of May and June in 2004 and SPL observation data for divalent mercury (Hg(II)) of May and June in 2000

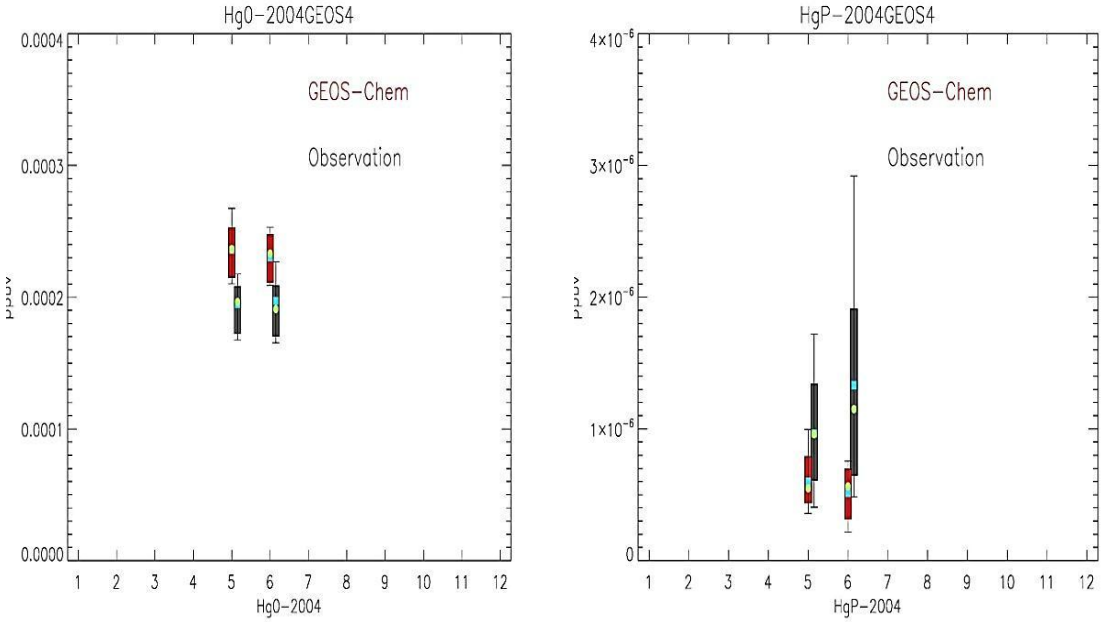

Figure.8, Comparison between GEOS-4 model simulation data for elemental mercury (Hg(0)) and primary particulate mercury (Hg(P)) of May and June in 2004 and SPL observation data for elemental mercury (Hg(0)) and primary particulate mercury (Hg(P)) of May and June in 2000

Looking further into this problem, we found one possible reason for high divalent mercury (Hg(II)) result from the model (Selin.2007). As shown in Figure.9, we can see the global annual mean mixing ratio of divalent mercury (Hg(II)) increases rapidly with altitude. This is mainly due to two reasons: the first is that there is sustained source of divalent mercury (Hg(II)) from elemental mercury (Hg(0)) oxidation in the high-altitude air; the second is that the sinks of divalent mercury (Hg(II)) from deposition and in cloud photoreduction are less efficient in the high-altitude air. To conclude, the model also predicts high surface divalent mercury (Hg(II)) concentration over elevated land and over continental deserts where deep vertical mixing brings high-altitude air to the surface. The SPL where the data come from is a mountain-top facility with 3220 meters altitude, so it is definitely elevated land. This analysis from Selin.2007 paper might be suitable for the high divalent mercury (Hg(II)) model result problem here.

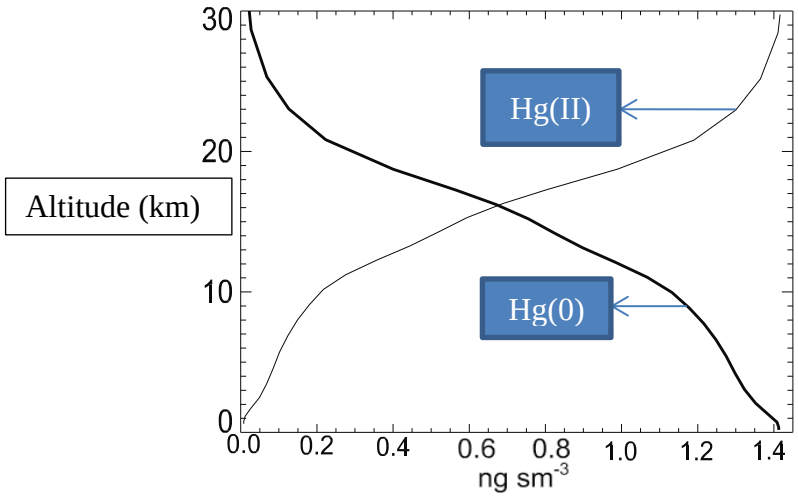

Figure.9, the global annual mean vertical profiles of elemental mercury (Hg(0)) and divalent mercury (Hg(II)) (Selin.2007)

After the two steps of model data verification above, we get the conclusion that the GCAP model simulation works normally.

2.3.Mercury Emissions

In our model GEOS-Chem, direct emissions of Hg(II) and Hg(P) in Geos-Chem are entirely of anthropogenic origin, while emissions of Hg(0) are from both natural and anthropogenic sources (Schroeder and Munthe, 1998). From the code file 'mercury_mod.f' in the model, we can see detailed mechanisms for the emissions of Hg(0), Hg(II) and Hg(P) in our GEOS-Chem model. The subroutine 'EMISSMERCURY' is the driver routine for mercury emissions. Since all the anthropogenic emissions are read from disk of the model, the direct emissions of Hg(II) and Hg(P) in Geos-Chem are offline simulation. For the computed Hg(0) emissions from natural sources , they consist of ocean emissions, biomass burning emissions, vegetation emissions, soil emissions, emissions from snow and ice and land reemissions. All the emissions of Hg(0) will be distributed throughout the boundary layer.

The ocean emissions of the Hg(0), which is included in the code file 'ocean_mercury_mod.f' in the model, is basically to compute the flux of Hg(0) from the ocean. The net flux, symbol F is expressed by the equation.1 below.

$$F = Kw * (Caq - \frac{Cg}{H})$$ (Xu et al, 1999) (Equ.1)

Kw is the exchange parameter, unit in cm/h, detailed calculation as shown in the equation.2.

$$Kw = 0.25 * u^2 / \sqrt{\frac{Sc}{ScCO_2}}$$(Nightingale, 2000) (Equ.2)

u is the wind speed (10m above ground) (m/s)

Sc is the Schmidt number which is unitless for elemental mercury (Hg(0)), detailed calculation as shown in the equation.3.

$Sc = \frac{nu}{D} = (0.017 * \exp(-0.025T))/(6.0 * 10^{-7} * T + 10^{-5})$ (Lin and Tao, 2003 and Poissant et al., 2000) (Equ.3)

T is temperature in degree C.

$ScCO_2$ is the Schmidt number for CO_2 at 20 degree C.

Caq is the surface water concentration, 1.5pM (Lamborg et al., 2002)

Cg is the gas-phase concentration

H is the dimensionless Henry coefficient for elemental mercury, the calculation for H is as shown in the equation.4.

$$H = exp(4633.3/T - 14.52)$$(Clever et al., 1985) (Equ.4)

T is sea temperature in Kelvin

As the calculations in Equation.1 to 4 showing, the exchange parameter Kw depends on T and u. As the T increases, Sc for elemental mercury (Hg(0)) decreases so that the exchange parameter Kw increases. As the u increases, the exchange parameter Kw increases. The dimensionless Henry coefficient H for elemental mercury depends on T. As T increases, H decreases. So the net flux F depends on T and u. An increasing u will cause an increasing net flux F, meanwhile an increasing T can lead the net flux F either increase or decrease.

For the biomass burning emissions of the Hg(0), which is included in the code file 'land_mercury_mod.f' in the model, is functioned by subroutine "BIOMASSHG (EHg0_bb)". It is based on an inventory of CO emissions from biomass burning, multiplied by an Hg/CO ratio (from Franz Slemr poster, EGU 2006). Slemr surveyed emission factors from measurements worldwide. In the GEOS-Chem simulation, the highest value (2.1e-7 mol Hg/mol CO) of the Hg/CO ratio in the range is used to do the

computation although the best estimate from Slemr was 1.5e-7 mol Hg/mol CO. The major reason for using the highest value is that the simulations shown in Selin et al.2008 required large Hg(0) emissions to sustain reasonable atmospheric Hg(0) concentrations. To conclude, the biomass burning emissions of the Hg(0) only depends on the biomass burning CO emissions since the Hg/CO ratio in the model is a constant. An increasing biomass burning CO emissions will lead to an increasing biomass burning emissions of the Hg(0).

The Hg(0) emissions from vegetation by evapotranspiration, which is also included in the code file 'land_mercury_mod.f' in the model, is functioned by subroutine "VEGEMIS(LGCAPEMIS, EHg0_dist, EHg0_vg)". Vegetation emissions are proportional to the evapotranspiration rate and the soil water mercury content. The GEOS-Chem model assumes a constant concentration of mercury in soil matter, based on the preindustrial and present-day simulations described in Selin et al.2008 and in "SOILEMIS" subroutine. From the soil matter mercury (Hg) concentration, we calculate a soil water mercury (Hg) concentration in equilibrium (Allison and Allison, 2005). The monthly average transpiration rate [m/s] used in the model is from NASA. The vegetation emissions of Hg(0) is calculated as shown in equation.5 below.

$$Fc = Ec * Cw$$ (Xu et al., 1999)(Equ.5)

Fc is Hg(0) flux of vegetation emissions, in ng/(m^2s).

Ec is canopy transpiration rate, in m/s

Cw is the concentration of Hg(0) in surface soil water (ng/m^3), the calculation of Cw is shown in equation.6 below.

$$Cw = Cs/Kd$$ (Allison and Allison (2005) equilibrium formula)(Equ.6)

Cs is the concentration of Hg(0) in surface soil solids, ng/g

Kd is the equilibrium constant = (sorbed)/ (dissolved) =6310 L /kg

To conclude, as we can see from the equation.5, the Fc (Hg(0) flux of vegetation emissions) depends on Ec (canopy transpiration rate) and Cw (the concentration of Hg(0) in surface soil water). Since the Ec (canopy transpiration rate) value in the model simulation process is a constant, the only changing factor for the Fc (Hg(0) flux of vegetation emissions) is Cw. From equation.6 above, Cw (the concentration of Hg(0) in surface soil water) depends on Cs (the concentration of Hg(0) in surface soil solids) and Kd (the equilibrium constant). As Kd is another constant, Cw is only affected by Cs. So, the Fc (Hg(0) flux of vegetation emissions) is only proportional to Cs (the concentration of Hg(0) in surface soil solids).

There is another kind of Hg(0) emissions included in the model which is from soils. The soil Hg(0) emissions are also included in the code file 'land_mercury_mod.f' in the model, is functioned by subroutine "SOILEMIS(EHg0_dist, EHg0_so)" from that file. Soil emissions are a function of solar radiation at ground level (accounting for attenuation by leaf canopy) and surface temperature. The radiation dependence from Zhang et al. (2000) is multiplied by the temperature dependence from Poissant and Casimir (1998). Finally, this emission factor is multiplied by the soil mercury concentration and scaled to meet the global emission total. Present-day soil concentrations are thought to be 15% greater than preindustrial one which is 45 ng Hg /g dry soil. But such a difference is much less than the range of concentrations found today, so not well constrained. The GEOS-Chem model calculates the present-day soil mercury (Hg) distribution by adding a

global mean 6.75 ng/g (=0.15 * 45 ng/g) according to present-day mercury (Hg) deposition.

For summary, as the fraction of light reaching the surface (attenuate solar radiation) is getting more, the Hg(0) emissions from soils are increasing. Theoretically, the soil emissions of Hg(0) is an exponential function of both soil temperature and solar radiation. This is also the reason for the strong summer peak of the Hg(0) emissions from soils. However in the GEOS-Chem model, the soil emissions of Hg(0) is only proportional to exp(Rg). Rg is solar radiation flux at the ground. So, the solar radiation flux at the ground increases, the Hg(0) emissions from soils are increasing.

The model also includes the emission of Hg(0) from snow and ice even though they are very small source of mercury emissions. Some of the mercury deposited reemit from sunlit snow packs in spring and summer due to snowmelt (Holmes, 2010). These emissions are a linear function of mercury mass stored in the snowpack. The mercury lifetime in snow is assumed to be 180 days when the temperature is less than 270 Kelvin degrees and 7 days when the temperature is greater than 270 Kelvin degrees.

The last part of the computed Hg(0) emissions from natural sources is land reemission. It is the emissions of Hg(0) from prompt recycling of previously deposited mercury to land which is included in the subroutine “LAND_MERCURY_FLUX”. In the GEOS-Chem model, land reemission of Hg(0) is proportional to the sum of total deposition of Hg(II) and Hg(P) for both wet and dry depositions. There is a reemission fraction which is 0.6 if the snow depth is greater than 1mm on the ground, otherwise it is 0.2.

For the anthropogenic emissions in both Present-day (2000) and future (2050), we use the Global Emission Inventory Activity (GEIA) global inventory of anthropogenic emissions

for 2000. This inventory includes Hg(0), Hg(II) and Hg(P) at 1278, 720, and 192 Mg yr-1, respectively, with a horizontal resolution of 1 by 1 and no seasonal variation. For the GCAP (Global Change and Air Pollution) use by our Geos-Chem model, the emission files are created on 72×45 grids, different from the 72×46 grids used in GEOS-5 simulations. Major sources in that inventory are electric power generation and waste incineration. Mobile sources are not consistently included, although recent data suggest that they could be significant (Edgerton and Jansen, 2004; Lynam and Keeler, 2006). The global emission rate of anthropogenic mercury declined by 5.5% from 1995 to 2000 according to GEIA, but there have been more substantial regional changes. Emissions in the United States and Russia declined by 12% and 46%, respectively, while emissions in India, Brazil, Mexico, and Spain increased. Emissions in China declined 1.9%. Asia accounted for 54% of global anthropogenic mercury emissions in 2000.

In the atmosphere, the Hg(0)'s resident time is about one year due to its relatively slow oxidation to the mercuric state (divalent mercury). This time is sufficient time for atmospheric mercury to be distributed over the entire planet before returning to the land, lakes, sea, and ice. So, while the principal emissions of mercury are from some point sources concentrated in industrial regions, the mercury pollution is getting globally, affecting the most remote areas of the world. And the troposphere provides effective global transport of Hg(0).

2.4.Mercury Chemistry

In the atmosphere, mercury can equilibrate among gaseous, aqueous and solid phases. Atmospheric mercury can undergo various physical and chemical transformations before being deposited back to the ground. Atmospheric mercury exists primarily as inorganic

forms with two oxidation states: Hg(0) and Hg(II), although the existence of methylated mercury has also been reported (<3% of the total gaseous Hg except at near emissions sources, Slemr et al., 1985; Fitzgerald et al., 1991; Lee and Iverfeldt, 1991; Lamborg et al., 1995; St. Louis et al., 1995). The chemistry of atmospheric mercury was first reviewed by Lindqvist and Rodhe (1985). They suggested that photochemical processes may be important for the production of Hg(II) species in the atmosphere, and that the presence of water seems to accelerate Hg(0) oxidation, although no specific reaction pathways were discussed (Lindqvist and Rodhe (1985)). After this first review of the chemistry of atmospheric mercury, several other reviews of the chemistry of atmospheric mercury had been done during the coming years. The objective of these reviews is to summarize the understanding of atmospheric mercury chemistry, because many more reaction pathways and kinetic data have become available since the work by Lindqvist and Rodhe (1985).

In our work, we focus on the atmospheric mercury concentration change from 2000 to 2050, so special attention is paid to the kinetics, mechanisms and implications of the reactions interconverting Hg between elemental and divalent states. Most of these reactions were proposed to take place in atmospheric water.

Among atmospheric mercury transformation reactions between elemental and divalent states, there are three major oxidation pathways (Hg(0) by ozone, Hg(0) by OH, Hg(0) by HOCl/OCl) which stands for Hg(0) oxidation to Hg(II) and also three major reduction pathways (Hg(II) by SO_3, Hg(II) by HO_2, Hg(II) photoreduction) which stands for Hg(II) reduction to Hg(0).

The model does not include all those oxidation and reduction pathways showing above, instead, GEOS-Chem only includes the most major pathway for either oxidation or reduction. The model includes Hg(0) oxidation to Hg(II) by OH (Pal and Ariya, 2004a;Sommar et al., 2001) and ozone (Hall, 1995). There are no temperature dependence is included in these rate constants due to lack of data. Oxidation rates are calculated using archived monthly mean 3-D fields of OH and O3 concentrations from a detailed GEOS-Chem tropospheric chemistry simulation (Park et al., 2004). The chemical speciation of Hg(II) measured in the atmosphere as RGM is unknown (Mason and Sheu, 2002); the Hg(II) product of the reactions of Hg(0) with O3 and OH is likely HgO (Sommar et al., 2001). HgO is very soluble in water thus dissolves in aqueous aerosols and clouds (Schroeder and Munthe, 1998). In the aqueous phase, HgO dissociates to Hg^{2+} (Pleijel and Munthe, 1995). Under most atmospheric conditions, Cl concentrations in the aqueous phase are sufficiently high to drive recomplexation to $HgCl_2$ (Lin and Pehkonen, 1998). For reduction, the model includes the aqueous-phase photoreduction of Hg(II) as the only reduction pathway. In the model, this photoreduction pathway is based on estimate of rate constant and scaled to OH concentration. As same as the oxidation pathway above, there are No temperature dependence is included in these rate constants due to lack of data. Reduction rates are also calculated using archived monthly mean 3-D fields of OH concentration from a detailed GEOS-Chem tropospheric chemistry simulation (Park et al., 2004). The model also includes the sum of oxidation of Hg(0) and reduction of Hg(II) which is production of Hg(II) from Hg(0).

2.5.Mercury Deposition

The GEOS-Chem model simulates both wet and dry deposition fluxes for divalent mercury (Hg(II)) and primary particulate mercury (Hg(P)) but only dry deposition flux for elemental mercury (Hg(0)) (Selin and Jacob 2008). The reason is that the Henry's law constant of elemental mercury (Hg(0)) is very low (0.11 M atm-1 at 298K (Lin and Pehkonen, 1999)). From the Global atmospheric mercury budget in GEOS-Chem model showing in the Figure.20 below, we can see the numbers of deposition amount for the three different mercury species included in the model: elemental mercury (Hg(0)), divalent mercury (Hg(II)) and primary particulate mercury (Hg(P)), respectively. For divalent mercury (Hg(II)), the total deposition amount is largest among the three tracers while the dry deposition dominates over the wet deposition (dry deposition:4700 Mg/year, wet deposition: 2100 Mg/year) (Selin.2007). The dry deposition amount of primary particulate mercury (Hg(P)) is almost neglected since the wet deposition is 190 Mg/year while the dry deposition is only 10 Mg/year (Selin.2007). The most deposition of elemental mercury (Hg(0)) happens after the oxidation of elemental mercury (Hg(0)) to divalent mercury (Hg(II)). So, there is no specific deposition amount of elemental mercury (Hg(0)) included in GEOS-Chem model (Selin.2007).

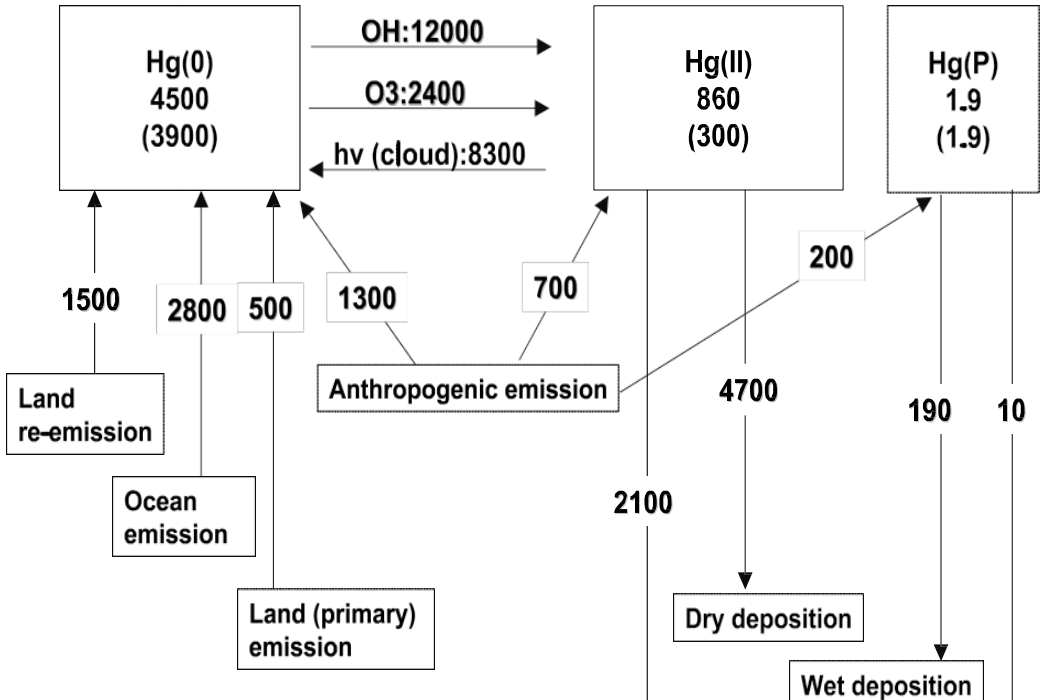

Figure.20, the Global present-day atmospheric mercury budget in GEOS-Chem model for version 8-03-01 (Selin.2007)

In our work, we make the plots of wet deposition flux for 2000 and 2050 for divalent mercury (Hg(II)) and primary particulate mercury (Hg(P)) to see the difference of wet deposition flux between 2000 and 2050 due to the climate change from 2000 to 2050. What is more, the deposition flux of mercury is an important factor which can affect the surface concentration of mercury. So the difference of wet deposition flux between 2000 and 2050 could be a reason for the surface concentration changes of mercury.

The wet deposition in GEOS-Chem model includes rainout and washout from large-scale and convective precipitation, and scavenging in convective updrafts (Liu et al., 2001). We assume that divalent mercury (Hg(II)) is scavenged quantitatively by liquid precipitation but is released to the gas phase when water freezes (zero retention efficiency). Primary particulate mercury (Hg(P)) is scavenged with the same efficiency as a water soluble aerosol (Liu et al., 2001). Dry deposition simulation included in the GEOS-Chem model is represented by the dry deposition flux density (F), which equals to deposition velocity (V) times the concentration (C). As a result, the higher concentrations of the mercury species in the air will lead to the higher dry deposition flux density (F) of them, respectively. Globally, the mean percentage of total deposition from a source is

equivalent to its contribution to emission. However, the percentage varies spatially; contributions of emissions sources to deposition in a particular location depend on both the species of mercury (Hg) emitted and atmospheric chemical processes, transport, and circulation patterns.

3. Results Discussion

3.1 Impacts of 2000-2050 climate change on mercury in the atmosphere

The Figure.10 shows the simulated result by GCAP for 3-year average Hg(0) concentration for year 2000 and year 2050, respectively in the top panel and the Hg(0) concentration difference by (2050-2000) and (2050-2000)/2000 percentage in the bottom panel. This Figure examines more specifically the change in the global distribution of Hg(0) (3-year mean concentrations). Since we use the Global Emission Inventory Activity (GEIA) global inventory of anthropogenic emissions for the year 2000 for Present-day (2000) and the future (2050), the change in the global distribution of Hg(0) surface concentration from 2000 to 2050 is due to the climate change. From the (2050-2000) concentration difference plot in the bottom panel, we can see that change in climate decrease Hg(0) surface concentration in most of the world, except in some regions, north-eastern of China, south-eastern of South Africa and central part of Europe. This surface concentration decline of the elemental mercury (Hg(0)) could be due to either decreasing sources or increasing sinks of the surface elemental mercury (Hg(0)). From the Global atmospheric mercury budget included in the GEOS-Chem model (Selin.2007), we can get that there is no specific deposition pathway for elemental mercury (Hg(0)) which means the dry deposition sink of elemental mercury (Hg(0)) could be treated neglected in GEOS-Chem simulations. As a result, the major sink of the

atmospheric elemental mercury (Hg(0)) is just the oxidation to divalent mercury (Hg(II)) as described in ‘Mercury Chemistry’ section above. Also from the Global atmospheric mercury budget included in the GEOS-Chem model (Selin.2007), we can see the major sources of the atmospheric elemental mercury (Hg(0)) are reduction from divalent mercury (Hg(II)) and emissions which is the sum of anthropogenic emissions and natural emissions. Since the GEOS-Chem model includes Hg(0) emissions from both natural and anthropogenic sources (Schroeder and Munthe, 1998), the natural emissions of elemental mercury (Hg(0)) decreases could be one possible reason for the surface Hg(0) concentration decline in the blue regions as showing in Figure.10. As mentioned above in the “Mercury Emission” part, there are different kinds of computed Hg(0) emissions from natural sources in the model. The blue areas above the marine part of earth surface might be due to reduced ocean emissions of the Hg(0). The reduced ocean emissions of the Hg(0) can happen by either decreasing wind speed over the ocean or temperature change. Hg(0) concentration changes can also be due to vegetation emissions changes as the concentration of Hg(0) in surface soil solids changes. What is more, as the solar radiation flux at the ground changes, the Hg(0) emissions from soils are changing. This change can also cause the Hg(0) concentration changes in the atmosphere (as the red and blue parts showing). Other than the mercury natural emissions impact, the transformation between elemental mercury (Hg(0)) and divalent mercury (Hg(II)) is also an important factor which is able to influence the surface concentration of elemental mercury (Hg(0)). Summary from above, either decreasing reduction from divalent mercury (Hg(II)) or increasing oxidation to divalent mercury (Hg(II)) could be another important factor for the surface concentration of elemental mercury (Hg(0)) decline.

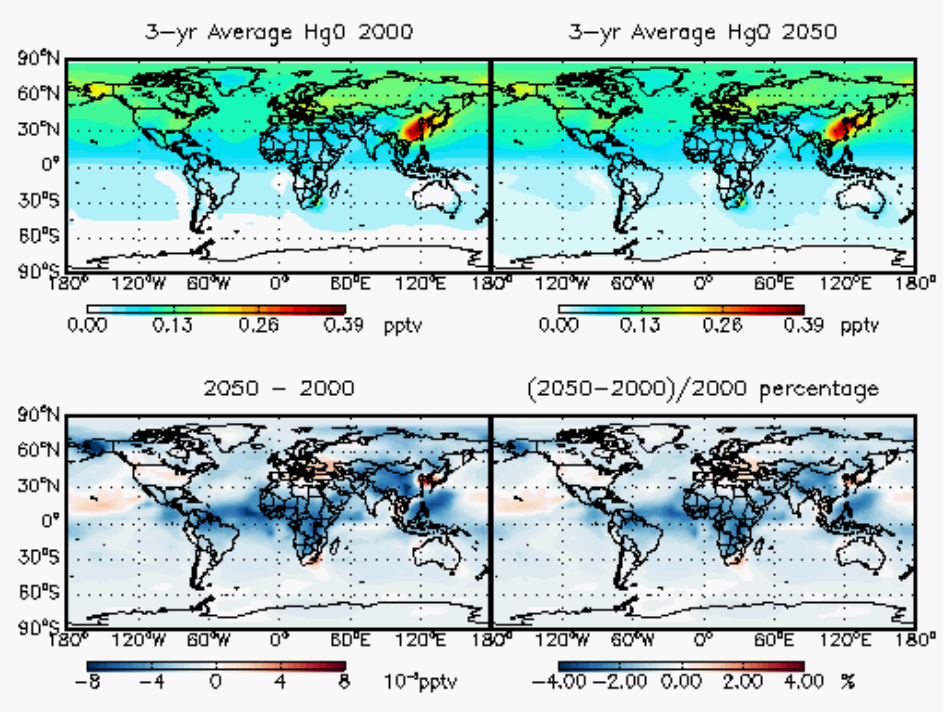

Figure.10, the 3-year average elemental mercury (Hg(0)) surface concentration for year 2000 and year 2050, the difference between (2050-2000) and (2050-2000)/2000 percentage

The Figure.11 shows the simulated result by GCAP for 3-year average divalent mercury (Hg(II)) surface concentration for 2000 and 2050, respectively in the top panel and the Hg(II) concentration difference by (2050-2000) and (2050-2000)/2000 percentage in the bottom panel. This figure examines more specifically the change in the global distribution of divalent mercury (Hg(II)) (3-year average concentrations). Since we use the Global Emission Inventory Activity (GEIA) global inventory of anthropogenic emissions for the year 2000 for Present-day (2000) and the future (2050), the change in the global distribution of divalent mercury (Hg(II)) surface concentration from 2000 to 2050 is due to the climate change. From the (2050-2000) concentration difference plot in the bottom panel, we can see that climate change affect the divalent mercury (Hg(II)) surface concentration in a much more complicated way than affect the elemental mercury

(Hg(0)) surface concentration. Climate change increase the divalent mercury (Hg(II)) surface concentration in most of mid-latitude continental parts of the world, such as the whole Africa continent and the major part of south Asia. At the same time, Climate change decrease the divalent mercury (Hg(II)) surface concentration in most of high-latitude part of the world. We can also see this point more clearly by using the (2050-2000)/2000 percentage plot in lower panel of Figure.11. By the same analysis method as used in the elemental mercury (Hg(0)) part above, the changes of the divalent mercury (Hg(II)) surface concentration are due to the sum changes of sources and sinks. From the Global atmospheric mercury budget included in the GEOS-Chem model (Selin.2007), we can see the major sources of divalent mercury (Hg(II)) are anthropogenic mercury emissions and oxidation from elemental mercury (Hg(0)) while the major sinks of divalent mercury (Hg(II)) are wet/dry depositions to the ground and reduction to elemental mercury (Hg(0)). As a result of analysis, the changes of transformation between elemental mercury (Hg(0)) and divalent mercury (Hg(II)) (either oxidation from elemental mercury (Hg(0)) or reduction to elemental mercury (Hg(0))) are able to cause the divalent mercury (Hg(II)) surface concentration differences between 2000 and 2050. The other important factor is the depositions amount of divalent mercury (Hg(II)). As mentioned in the ‘Mercury Deposition’ section above, the simulated dry deposition flux density (F) included in the GEOS-Chem model depends on deposition velocity (V) and the concentration (C) of the mercury species. As a result, a higher concentration of divalent mercury (Hg(II)) in the air will lead to a higher dry deposition flux density (F) of divalent mercury (Hg(II)). So, the dry deposition amount of divalent mercury (Hg(II)) could impact its atmospheric surface concentration after the divalent mercury (Hg(II))

surface concentration has been changed by other factors. Since divalent mercury (Hg(II)) has a pretty good water solubility, it can be deposited and scavenged by rain. As a result, wet deposition pathway is the major way for return of mercury (Hg) from the atmosphere to the earth's surface. For the wet deposition factor, it depends on precipitation amount. As a result, changes of the precipitation amount from 2000 to 2050 could cause the divalent mercury (Hg(II)) surface concentration differences between 2000 and 2050.

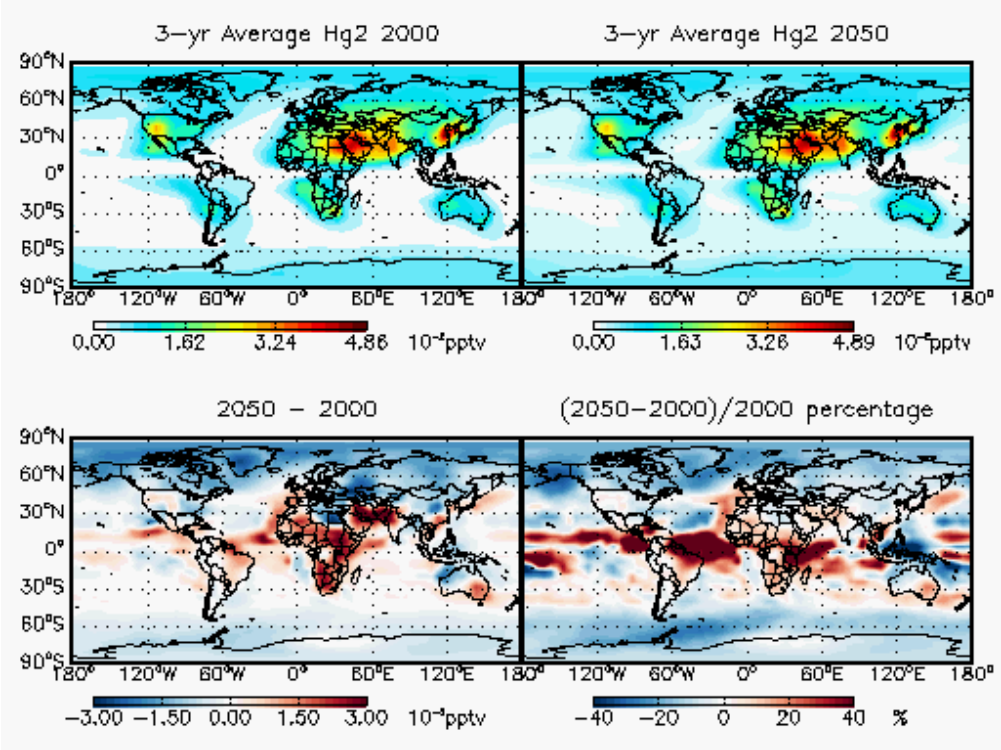

Figure.11, the 3-year average divalent mercury (Hg(II)) concentration for year 2000 and year 2050, the difference between (2050-2000) and (2050-2000)/2000 percentage

Since the factor of transformation between elemental mercury (Hg(0)) and divalent mercury (Hg(II)) plays an important role on surface concentration differences between 2000 and 2050 for both elemental mercury (Hg(0)) and divalent mercury (Hg(II)). We do the zonal mean difference plots for 3-year average elemental mercury (Hg(0)) and divalent mercury (Hg(II)) between 2000 and 2050 other than the surface layer plots of the

3-year average elemental mercury (Hg(0)) and divalent mercury (Hg(II)) concentration comparison between 2000 and 2050 as Figure.10 and 11 showing. From Figure.12 and 13, we can get the elemental mercury (Hg(0)) and divalent mercury (Hg(II)) concentration changes for altitude from surface up to 30 kilometers. The major conclusion we obtain from the difference plots in Figure.12 and 13 is that there must be some transformations between elemental mercury (Hg(0)) and divalent mercury (Hg(II)) during 2000 to 2050. The major increasing part for elemental mercury (Hg(0)) in Figure.12 is closely matching the major decreasing part for divalent mercury (Hg(II)) in Figure.13. In the same way, the major decreasing part for elemental mercury (Hg(0)) in Figure.12 is closely matching the major increasing part for divalent mercury (Hg(II)) in Figure.13. In order to look into the details of transformation between elemental mercury (Hg(0)) and divalent mercury (Hg(II)), we made the zonal mean difference plots between (2050-2000) for production of divalent mercury (Hg(II)) from elemental mercury (Hg(0)) as Figure.17 to 19 showing. Another motivation of making these plots is to get the proper reason for their transformation changes.

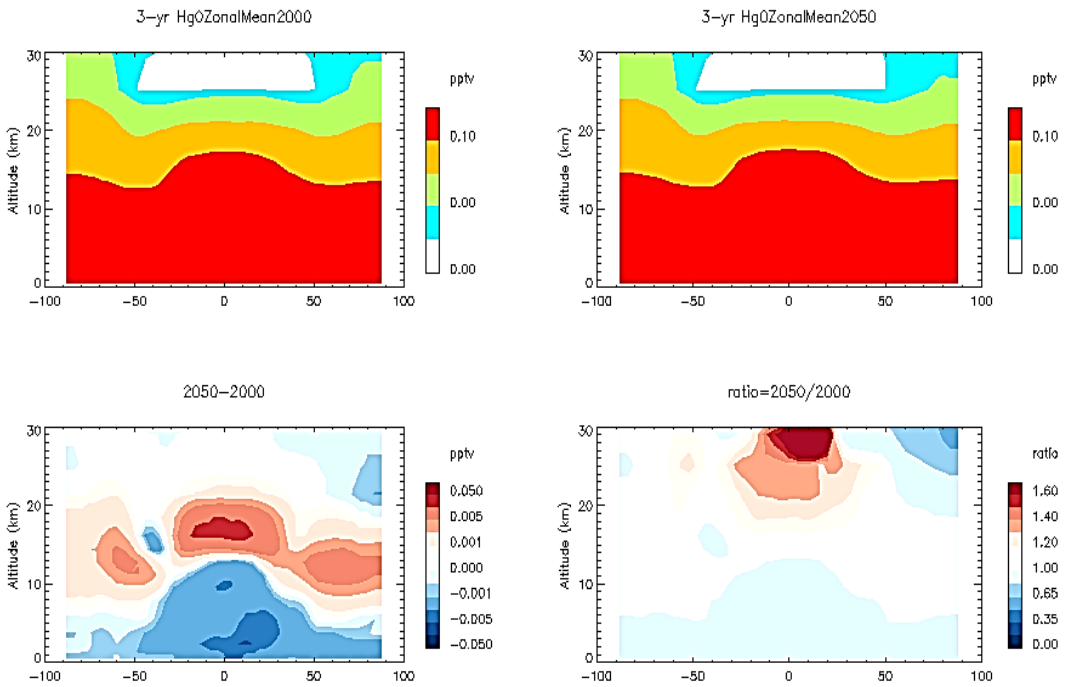

Fig.12. 3-year average zonal mean elemental mercury (Hg(0)) concentration for year 2000 and year 2050, the difference between (2050-2000) and the ratio 2050/2000

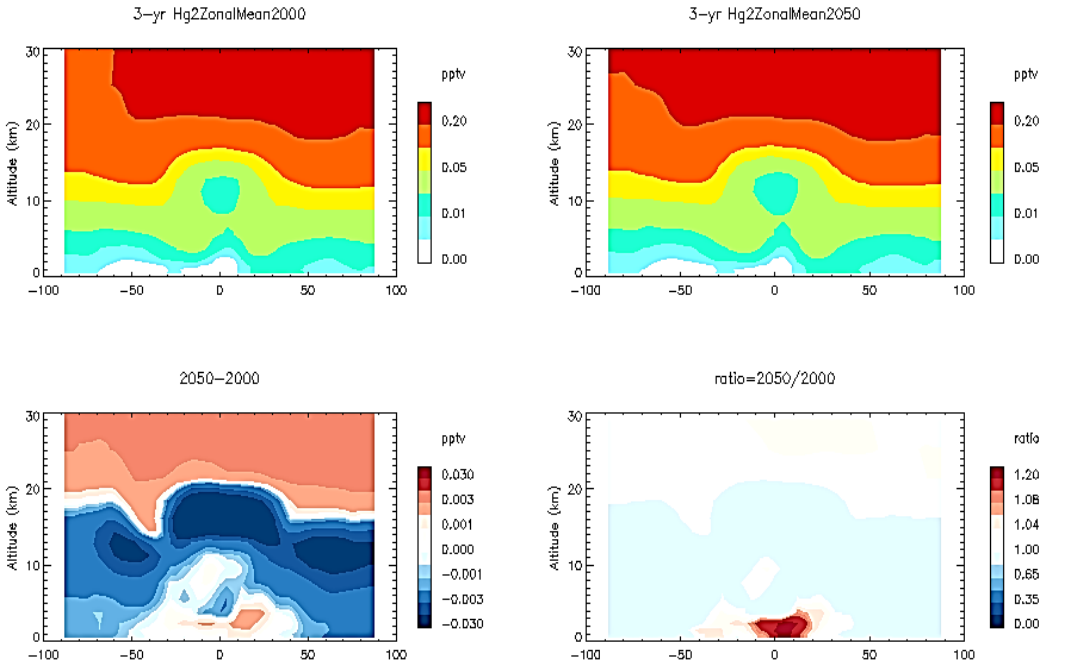

Fig.13. 3-year average zonal mean divalent mercury (Hg(II)) concentration for year 2000 and year 2050, the difference between (2050-2000) and the ratio 2050/2000

The Figure.14 shows the simulated result by GCAP for 3-year average Primary particulate mercury (Hg(P)) concentration for 2000 and 2050, respectively in the top panel and the Primary particulate mercury (Hg(P)) concentration difference by (2050-2000) and (2050-2000)/2000 percentage in the bottom panel. This Figure examines more specifically the change in the global distribution of Primary particulate mercury (Hg(P)) (3-year average concentrations). Since we use the Global Emission Inventory Activity (GEIA) global inventory of anthropogenic emissions of 2000 for both Present-day (2000) and the future (2050), the change in the global distribution of Primary particulate mercury (Hg(P)) surface concentration from 2000 to 2050 is due to the climate change. Climate change increases Primary particulate mercury (Hg(P)) concentration in most of mid-latitude area of the world and meanwhile decreases Primary particulate mercury (Hg(P)) concentration in most of high-latitude area of the world. From the (2050-2000) concentration difference plot in the bottom panel, we can see the absolute value of the (2050-2000) surface concentration difference of Primary particulate mercury (Hg(P)) is relative small in most of the world and there are only couple high values in south and east parts of China, south-eastern part of Australia, south Asia and South Africa. The (2050-2000) surface concentration differences of Primary particulate mercury (Hg(P)) are due to the sum changes of sources and sinks. Also from the Global atmospheric mercury budget included in the GEOS-Chem model (Selin.2007), we can see the source of Primary particulate mercury (Hg(P)) in the atmosphere is anthropogenic emissions while the sink of Primary particulate mercury (Hg(P)) are wet/dry depositions to the ground. Since we use the Global Emission Inventory Activity (GEIA) global inventory of anthropogenic emissions of 2000 for both Present-day (2000) and the future (2050), the

(2050-2000) surface concentration differences of Primary particulate mercury (Hg(P)) is totally due to change of sink which is wet/dry depositions. As same as divalent mercury (Hg(II)), Primary particulate mercury (Hg(P)) can also be deposited and scavenged by rain. As mentioned in the 'mercury deposition' part above, for Primary particulate mercury (Hg(P)), the wet deposition pathway dominates over the dry deposition one. As a result, the change of wet deposition amount from 2000 to 2050 is the dominating factor to impact the surface concentration changing of Primary particulate mercury (Hg(P)) from 2000 to 2050. The wet deposition amount of Primary particulate mercury (Hg(P)) depends on the precipitation amount. So, change of the precipitation amount from 2000 to 2050 can impact the surface concentration in the atmosphere of Primary particulate mercury (Hg(P)) from 2000 to 2050.

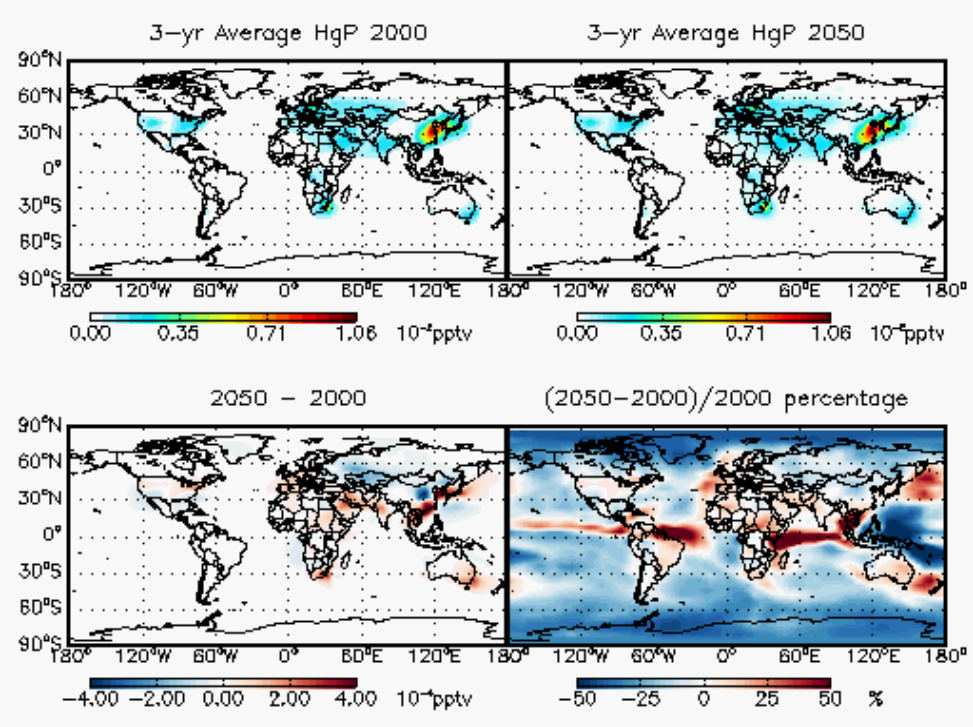

Fig.14. The 3-year average Primary particulate mercury (Hg(P)) concentration for year 2000 and year 2050, the difference between (2050-2000) and (2050-2000)/2000 percentage

3.2 Impacts of 2000-2050 climate change on mercury deposition

The Figure.15 shows the simulated result by GCAP for 3-year average divalent mercury (Hg(II)) wet deposition flux for 2000 and 2050, respectively in the top panel and the divalent mercury (Hg(II)) wet deposition flux difference by (2050-2000) and (2050-2000)/2000 percentage in the bottom panel. This Figure examines more specifically the change in the global distribution of divalent mercury (Hg(II)) wet deposition flux (3 years average). Since we use the Global Emission Inventory Activity (GEIA) global inventory of anthropogenic emissions for the 2000 for both Present-day (2000) and the future (2050), the change in the global distribution of divalent mercury (Hg(II)) wet deposition flux from 2000 to 2050 is due to the climate change. From the (2050-2000) divalent mercury (Hg(II)) wet deposition flux difference plot in the bottom panel, we can see that climate change from 2000 to 2050 will not affect the divalent mercury (Hg(II)) wet deposition flux in big scale. As mentioned in 'mercury deposition' section above, in the GEOS-Chem model, the simulation of wet deposition includes rainout and washout from large-scale and convective precipitation, and scavenging in convective updrafts (Liu et al., 2001). So change of the wet deposition flux here could be due to the change of precipitation amount from 2000 to 2050 or atmospheric concentration changes of divalent mercury (Hg(II)). As we obtain from Figure.15, the net change of the divalent mercury (Hg(II)) wet deposition flux from 2000 to 2050 is very small. The values in the (2050-2000) divalent mercury (Hg(II)) wet deposition flux difference plot are relatively small compared with the value of 2000 or 2050, also the (2050-2000)/2000 percentage values are almost neglected since the values are as small as 10^{-4} percent. As a result, in this case, the change of divalent mercury (Hg(II)) wet deposition flux from 2000 to 2050 is not the

major reason for the differences of divalent mercury (Hg(II)) surface concentration in the air between 2000 and 2050.

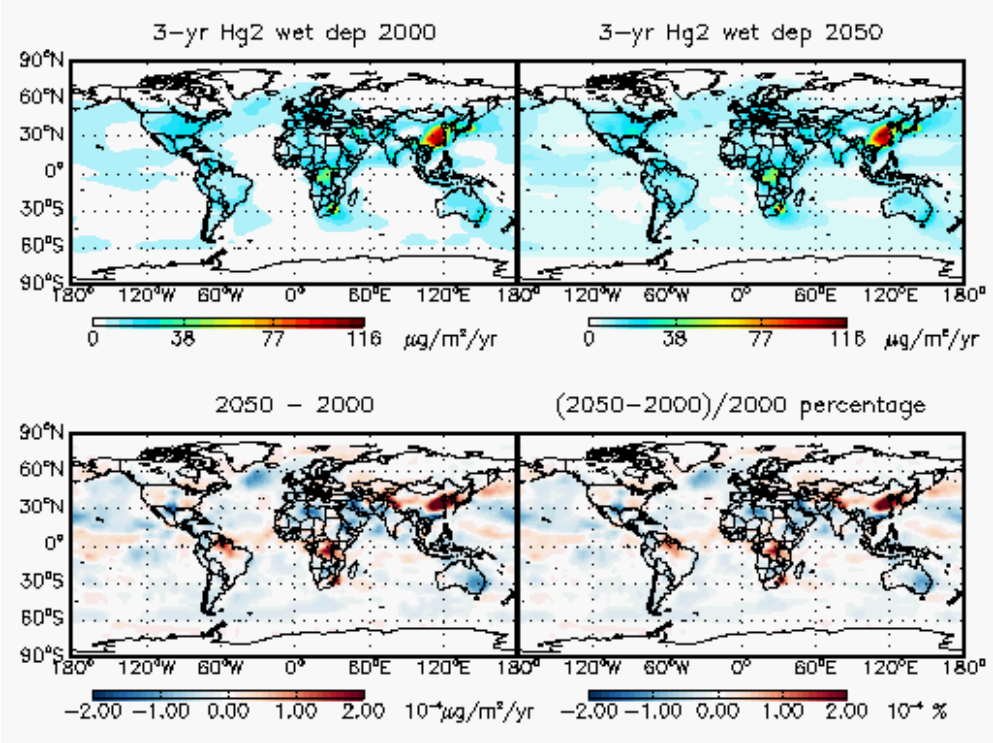

Fig.15. The 3-year average divalent mercury (Hg(II)) wet deposition flux for year 2000 and year 2050, the difference between (2050-2000) and (2050-2000)/2000 percentage

The Figure.16 shows the simulated result by GCAP for 3-year average Primary particulate mercury (Hg(P)) wet deposition flux for year 2000 and year 2050, respectively in the top panel and the primary particulate mercury (Hg(P)) wet deposition flux difference by (2050-2000) and (2050-2000)/2000 percentage in the bottom panel. This Figure examines more specifically the change in the global distribution of primary particulate mercury (Hg(P)) wet deposition flux (3 years average). Since we use the Global Emission Inventory Activity (GEIA) global inventory of anthropogenic emissions for the 2000 for both Present-day (2000) and the future (2050), the change in the global distribution of primary particulate mercury (Hg(P)) wet deposition flux from 2000 to

2050 is due to the climate change. From the (2050-2000) primary particulate mercury (Hg(P)) wet deposition flux difference plot in the bottom panel, we can see that change in climate from 2000 to 2050 will not affect the primary particulate mercury (Hg(P)) wet deposition flux in big scale. Very similar to divalent mercury, the primary particulate mercury (Hg(P)) is water soluble and its change of wet deposition amount from 2000 to 2050 is the dominating factor to impact the surface concentration changing of Primary particulate mercury (Hg(P)) from 2000 to 2050. However, the values in the (2050-2000) primary particulate mercury (Hg(P)) wet deposition flux difference plot are very small compared with the 2000 year or 2050 year values, also the (2050-2000)/2000 percentage values are almost neglected since the values are as small as 10^{-5} percent. This difference percentage of primary particulate mercury (Hg(P)) wet deposition flux is too small to explain the surface concentration changing of primary particulate mercury (Hg(P)) from 2000 to 2050 which is as high as a 50 percent change from Figure.14. So, future work is needed on this issue.

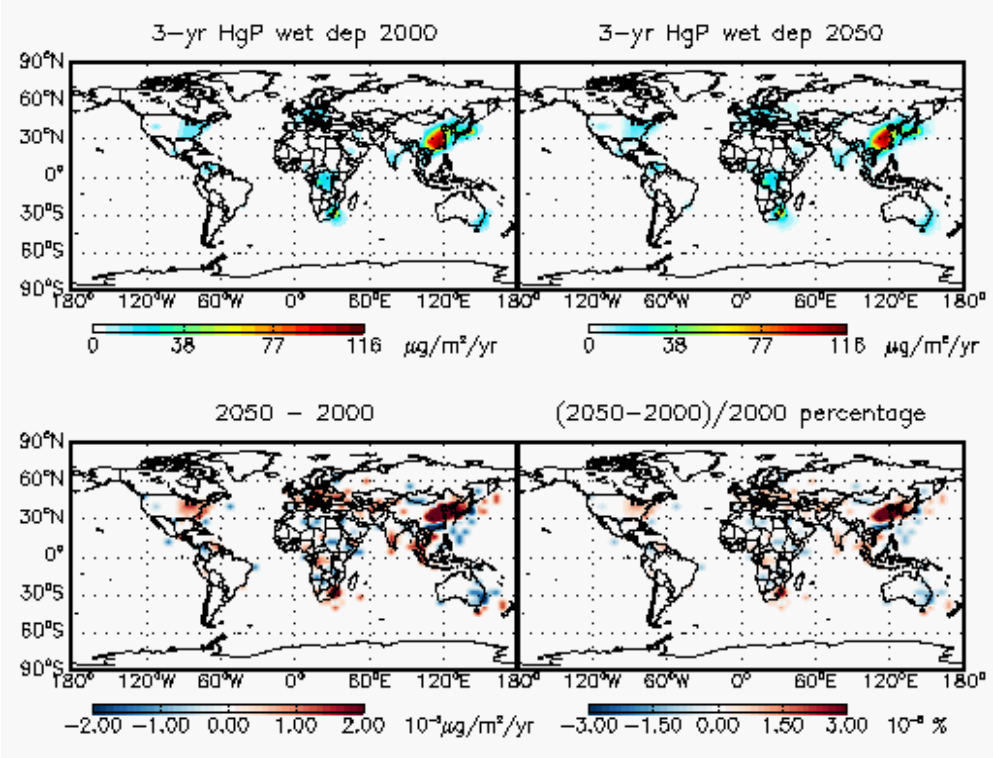

Fig.16. 3-year average primary particulate mercury (Hg(P)) wet deposition flux for year 2000 and year 2050, the difference between (2050-2000) and (2050-2000)/2000 percentage

3.3. Impacts of 2000-2050 climate change on atmospheric mercury chemistry

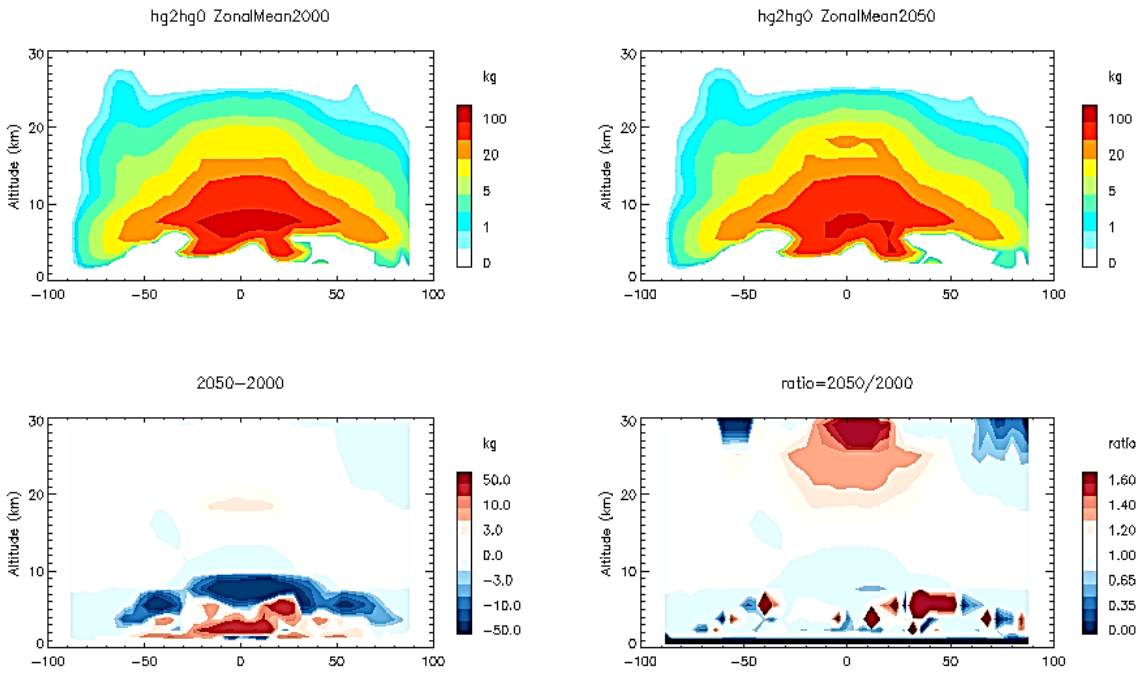

Fig.17. The 3-year average zonal mean plot for production of divalent mercury (Hg(II)) from elemental mercury (Hg(0)) for year 2000 and year 2050, the difference between (2050-2000) and the ratio 2050/2000

The Figure.17 shows the simulated result by GCAP for 3-year average production of divalent mercury (Hg(II)) from elemental mercury (Hg(0)) for year 2000 and year 2050, respectively in the top panel and production of divalent mercury (Hg(II)) from elemental mercury (Hg(0)) difference by (2050-2000) and the ratio 2050/2000 in the bottom panel. As mentioned above in the "Mercury Chemistry" section of this paper, there are several mercury transformation pathways between elemental and divalent states by either oxidation (elemental mercury (Hg(0)) convert to divalent mercury (Hg(II))) or reduction (divalent mercury (Hg(II)) convert to elemental mercury (Hg(0))). The production of divalent mercury (Hg(II)) from elemental mercury (Hg(0)) is the sum of oxidation of elemental mercury (Hg(0)) which is positive and reduction of divalent mercury (Hg(II)) which is negative. The model measures the production of divalent mercury (Hg(II)) from

elemental mercury (Hg(0)) by tracer No.35001 from ND03 diagnostic. As we can see from these zonal mean difference plots in the bottom panel, the most part of the lower atmosphere (troposphere (below 10km)) is showing blue which means decreasing for production of divalent mercury (Hg(II)) from elemental mercury (Hg(0)). But at the same time, for the surface layer which we care most, it is showing white and red which means production of divalent mercury (Hg(II)) from elemental mercury (Hg(0)) increasing, especially for the tropical region. This increasing of the divalent mercury (Hg(II)) production from elemental mercury (Hg(0)) explain the elemental mercury (Hg(0)) and divalent mercury (Hg(II)) surface concentration changing from 2000 to 2050 in Figure 10 and 11. As the divalent mercury (Hg(II)) production from elemental mercury (Hg(0)) increases, divalent mercury (Hg(II)) concentration will increase and elemental mercury (Hg(0)) concentration will decrease. Since the wet deposition flux difference plots in Figure 15 and 16 are showing so small changing from 2000 to 2050, the increasing of the divalent mercury (Hg(II)) production from elemental mercury (Hg(0)) showing in Figure 17 could be the most important reason for the elemental mercury (Hg(0)) and divalent mercury (Hg(II)) concentration changing from 2000 to 2050 in Figure 10 and 11.

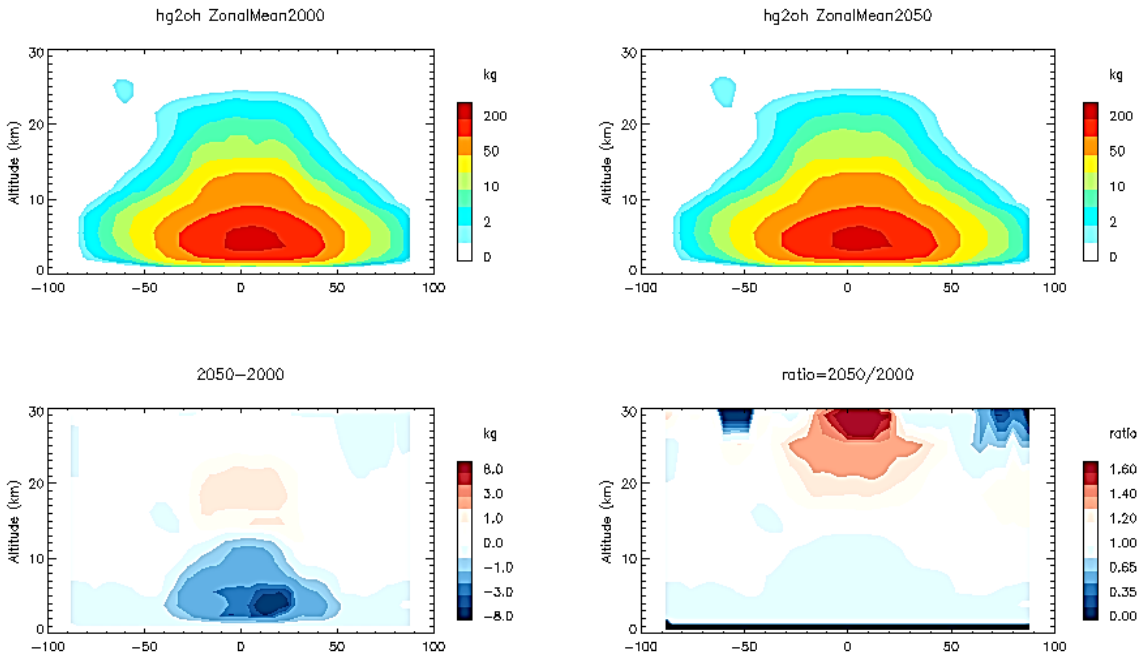

Fig.18. 3-year average zonal mean plot for production of Hg(II) from Hg(0) by OH for year 2000 and year 2050, the difference between (2050-2000) and the ratio 2050/2000

The Figure.18 shows the simulated result by GCAP for 3-year average production of Hg(II) from Hg(0) by OH for year 2000 and year 2050, respectively in the top panel and production of Hg(II) from Hg(0) by OH difference by (2050-2000) and the ratio 2050/2000 in the bottom panel. As mentioned above in the "Mercury chemistry" section of this paper, there are several mercury transformation pathways between elemental and divalent states by either oxidation (Hg(0) convert to Hg(II)) or reduction (Hg(II) convert to Hg(0)). The production of Hg(II) from Hg(0) is the sum of oxidation of Hg(0) which is positive and reduction of Hg(II) which is negative. The production of Hg(II) from Hg(0) by OH is one of two oxidation pathways included in the model that Hg(0) is oxidized by OH to convert to Hg(II). The model measures the production of Hg(II) from Hg(0) by OH by tracer No.35002 from ND03 diagnostic. As we can see from these zonal mean

difference plots in the bottom panel, values in the lower atmosphere (troposphere (below 10km)) is all showing blue by different degrees which means decreasing for production of Hg(II) from Hg(0) by OH. As mentioned above in "Mercury chemistry" section, the tracer No.35002, production of Hg(II) from Hg(0) by OH depends on archived monthly mean 3-D fields of OH concentration from a detailed GEOS-Chem tropospheric chemistry simulation (Park et al., 2004). So the OH concentration decreasing from 2000 to 2050 in that part of atmosphere is the only possible reason for the production of Hg(II) from Hg(0) by OH decreasing.

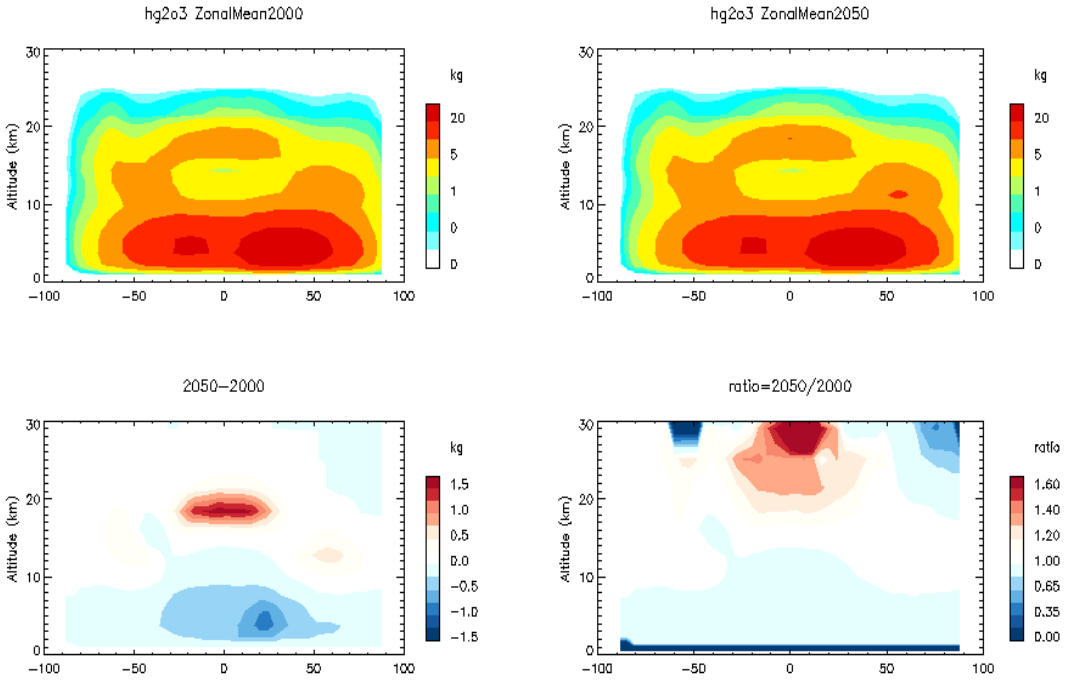

Fig.19. The 3-year average zonal mean plot for production of Hg(II) from Hg(0) by ozone for year 2000 and year 2050, the difference between (2050-2000) and the ratio 2050/2000

The Figure.19 shows the simulated result by GCAP for 3-year average production of Hg(II) from Hg(0) by ozone for year 2000 and year 2050, respectively in the top panel and production of Hg(II) from Hg(0) by ozone difference by (2050-2000) and the ratio

2050/2000 in the bottom panel. As mentioned above in the "Mercury Chemistry" section of this paper, there are several mercury transformation pathways between elemental and divalent states by either oxidation (Hg(0) convert to Hg(II)) or reduction (Hg(II) convert to Hg(0)). The production of Hg(II) from Hg(0) is the sum of oxidation of Hg(0) which is positive and reduction of Hg(II) which is negative. The production of Hg(II) from Hg(0) by ozone is one of two oxidation pathways included in the model that Hg(0) is oxidized by ozone to convert to Hg(II). The model measures the production of Hg(II) from Hg(0) by ozone by tracer No.35003 from ND03 diagnostic. As same as the Figure 13, from these zonal mean difference plots in the bottom panel, values in the lower atmosphere (troposphere (below 10km)) is all showing blue by same degree which means decreasing for production of Hg(II) from Hg(0) by ozone. As mentioned above in the "Mercury chemistry" section of this paper, the tracer No.35003, production of Hg(II) from Hg(0) by ozone depends on archived monthly mean 3-D fields of ozone concentration from a detailed GEOS-Chem tropospheric chemistry simulation (Park et al., 2004). So the ozone concentration decreasing from 2000 to 2050 in that part of atmosphere is the only possible reason for the production of Hg(II) from Hg(0) by ozone decreasing.

4. Conclusion

We have used a global 3-D atmospheric model (GEOS-Chem) to simulate three species of mercury in the atmosphere: elemental mercury (Hg(0)), divalent mercury (Hg(II)), and primary particulate mercury (Hg(P)) for two 3-year periods (1999-2001 and 2049-2051), with the first 3 years (1999-2001) used for getting the 3-year average value of Hg(0), Hg(II) and Hg(P), respectively in the year 2000 and the last 3 years (2049-2051) used for getting the 3-year average value of Hg(0), Hg(II) and Hg(P), respectively in the year

2050. The model version used in this research is “GCAP”. The research motivation is to see how the climate changes (year 2000 to year 2050) impact the mercury concentration in the atmosphere. We also includes the analysis of wet deposition fluxes of Hg(II) and Hg(P) comparison between present-day (2000) and the future (2050) since wet deposition flux is a very important indicator for the atmospheric concentration changes of Hg(II) and Hg(P) due to their strong solubility of water. And also to see how the climate changes from 2000 to 2050 impact the wet deposition fluxes of Hg(II) and Hg(P) in the atmosphere.

From the model results, we conclude that the model simulates the global atmospheric mercury (Hg) reasonably well. The climate change from 2000 to 2050 would decrease Hg(0) surface concentration in most of the world, only except in couple very small parts, for example north-eastern of China, south-eastern of South Africa and central part of Europe. The driving factors of Hg(0) surface concentration changes are natural emissions(ocean and vegetation) and the transformation reactions between Hg(0) and Hg(II). The climate change from 2000 to 2050 would increase Hg(II) surface concentration in most of mid-latitude continental parts of the world, such as the whole Africa continent and the major part of south Asia. At the same time, decrease Hg(II) surface concentration in most of high-latitude part of the world. The driving factors of Hg(II) surface concentration changes is deposition amount change (majorly wet deposition) from 2000 to 2050 and the transformation reactions between Hg(0) and Hg(II). Since Hg(II) has good water solubility, it can be deposited and scavenged by rain. The return of mercury from the atmosphere to the earth’s surface occurs majorly via wet precipitation of the dissolved Hg. For the Hg(P), we can see that a change in climate from

2000 to 2050 will affect the Hg(P) concentration in a very similar way as it will affect the Hg(II) concentration. It would increase Hg(P) concentration in most of mid-latitude area of the world and meanwhile decrease Hg(P) concentration in most of high-latitude regions of the world. For the Hg(P) concentration changes, the major driving factor is the deposition amount change (mainly wet deposition) from 2000 to 2050. Since Hg(P) is scavenged with the same efficiency as a water soluble aerosol as Hg(II) (Liu et al., 2001), it can also be deposited and scavenged by rain.

From wet deposition fluxes plots of Hg(II) and Hg(P), climate change from 2000 to 2050 will not affect the wet deposition flux of Hg(II) and Hg(P) in big scale. The values in the (2050-2000) wet deposition flux of Hg(II) and Hg(P) difference plot are relatively small compared with the 2000 year or 2050 year values, therefore the (2050-2000)/2000 percentage values are almost neglected.

5. Issues/Future work

As mentioned in research motivation part above, we were planning to make the comparison for global atmospheric mercury budget (as showing in Figure.20 for present-day) between present-day and future. However, the model GEOS-Chem in version 8-03-01 was not able to save the ND44 values for mercury simulations which are the dry deposition fluxes for mercury (Hg). As a result, we are not able to compare the global atmospheric mercury budget (as showing in Figure.20 for present-day) between present-day and future. The future work from my suggestion is using the updated version of model (newer than v9-01-01) to recompile and run this mercury simulation so as to get the ND44 values for dry deposition fluxes.

6. Acknowledgements

The author would like to thank Dr. Shiliang Wu for the help, encouragement, and instruction along the “two years journey” for my master’s degree. Special thanks are also owed to Bob Page and Mackenzie Roser for their help with GEOS-Chem and IDL. Also thank the members of the MTU GEOS-Chem users group for their encouragement and help, including: Mark Weise, Yaoxian Huang, Huanxin Zhang, Aditya and Xueling. Last but not least, I would like to thank my housemates Xu Zhang and Wensheng Sun, for their support and encouragement.

References:

- Holmes, C.D., D.J. Jacob, E.S. Corbitt, J. Mao, X. Yang, R. Talbot, and F. Slemr, *Global atmospheric model for mercury including oxidation by bromine atoms*, Atmospheric Chemistry and Physics, 10, 12,037-12,057, 2010
- Allison, J. D., and T. L. Allison (2005), *Partition coefficients for metals in surface water, soil and waste*, Rep. EPA/600/R-05/074, U.S. Environ. Prot. Agency, Off. of Res. and Dev., Washington, D.C.
- Martinez-Cortizas, A., Pontevedra-Pombal, X., Garcia-Rodeja, E., Novoa-Munoz, J.C. and Shotyk, W., *Mercury in a Spanish Peat Bog: Archive of Climate Change and Atmospheric Metal Deposition*, Science, May 7, 1999.
- Jozef M.Pacyna, Elisabeth G. Pacyna, Frits Steenhuisen and Simon Wilson, *Global Anthropogenic emissions of mercury to the atmosphere,* The Encyclopedia Of Earth, August 29, 2008
- Selin, N.E. and D.J. Jacob. *Seasonal and spatial patterns of mercury wet deposition in the United States: North American vs. intercontinental sources*, Atmospheric Environment, 42, 5193-5204, 2008.
- Selin, N.E., D.J. Jacob, R.M. Yantosca, S. Strode, L. Jaegle, and E.M. Sunderland, *"Global 3-D land-ocean-atmosphere model for mercury: present-day vs. pre-industrial cycles and anthropogenic enrichment factors for deposition"*, Global Biogeochemical Cycles , 22, GB2011.
- Selin, N.E., D.J. Jacob, R.J. Park, R.M. Yantosca, S. Strode, L. Jaegle, and D. Jaffe, *Chemical cycling and deposition of atmospheric mercury: Global constraints from observations*, J. Geophys. Res, 112, DO2308, doi:10.1029/2006JD007450, 2007
- GEOS-Chem model details introduction in Harvard University website: (http://acmg.seas.harvard.edu/geos/)
- The fish consumption advisories for USA in EPA website: (http://www.usgs.gov/themes/factsheet/146-00/fig4b.gif)
- Schroeder, W. H., and J. Munthe (1998), Atmospheric mercury—An overview, Atmos. Environ., 32, 809–822.
- Xiaohong Xu, Xiusheng Yang, David R. Miller, Joseph J. Helble, Robert J. Carley, *Formulation of bi-directional atmosphere-surface exchanges of elemental mercury,* Atmospheric Environment, 33(1999) 4345-4355, 1998
- Philip D. Nightingale, Gill Malin, Cliff S. Law, Andrew J. Watson, Peter S. Liss, Malcolm I. Liddicoat, Jacqueline Boutin, Robert C. Upstill-Goddard, *In situ evaluation of air-sea gas exchange parameterizations using novel conservative and volatile tracers*, GLOBAL BIOGEOCHEMICAL CYCLES, VOL. 14, NO. 1, PP. 373-387, 2000

- X. Lin and Y. Tao, *A numerical modelling study on regional mercury budget for eastern North America,* Atmos. Chem. Phys., 3, 535–548, 2003
- Lamborg, C. H., W. F. Fitzgerald, J. O'Donnell, and T. Torgersen (2002), *A non-steady-state compartmental model of global-scale mercury biogeochemistry with interhemispheric gradients*, Geochim. Cosmochim. Acta, 66, 1105–1118.
- Edgerton, E. S., and J. J. Jansen (2004), *Elemental Hg measurements in Atlanta, GA, USA: Evidence for mobile sources?* paper presented at 7th International Conference on Mercury as a Global Pollutant, RMZ-Mater. and Geoenviron., Ljubljana, Slovenia.
- Lindqvist, O. and Rodhe, H. (1985). *Atmospheric mercury – a review*. Tellus 37B, 134.
- Slemr, F., Schuster, G., and Seiler, W., *Distribution, speciation, and budget of atmospheric mercury*, J. Atmos. Chem., 3, 407–434, 1985.
- Fitzgerald, L., Johnston, R., Brignall, T. J., Silvestro, R. and Voss, C., 1991. *Performance Measurement in Service Businesses*, C.I.M.A.
- Lee, Y.-H., and A. Iverfeldt. 1991. *Measurement of methylmercury and mercury in runoff, lake and rain waters.* Water Air Soil Pollut. 56:309–321.
- Lamborg, C.H., Fitzgerald, W.F., Vandal, G.M., Rolfhus, K.R., 1995. *Atmospheric mercury in northern Wisconsin: sources and species.* Water, Air, and Soil Pollution 80, 189–198.
- Nicole St-Louis, M.J.Dalton, S.V.Marchenko, A.F.J.Moffat and A.J.Willis, *The IUE Mega Campaign: Wind Structure and Variability of HD 50896 (WN5).* THE ASTROPHYSICAL JOURNAL, 452:L57–L60, 1995 October 10
- Pal, B., and P. A. Ariya (2004a), *Gas-phase HO-initiated reactions of elemental mercury: Kinetics and product studies, and atmospheric implications*, Environ. Sci. Technol., 38, 5555– 5566.
- Sommar, J., K. Gardfeldt, D. Stromberg, and X. Feng (2001), *A kinetic study of the gas-phase reaction between the hydroxyl radical and atomic mercury*, Atmos. Environ., 35, 3049– 3054.
- Hall, B. (1995), *The gas phase oxidation of elemental mercury by ozone*, Water Air Soil Pollut., 80, 301– 315.
- Park, R. J., D. J. Jacob, B. D. Field, R. M. Yantosca, and M. Chin (2004), *Natural and transboundary pollution influences on sulfate-nitrate-ammonium aerosols in the United States: Implications for policy*, J. Geophys. Res., 109, D15204, doi:10.1029/2003JD004473.
- Mason, R. P., and G.-R. Sheu (2002), *Role of the ocean in the global mercury cycle*, Global Biogeochem. Cycles, 16(4), 1093, doi:10.1029/2001GB001440.
- Pleijel, K., and J. Munthe (1995), *Modeling the atmospheric mercury cycle—Chemistry in fog droplets*, Atmos. Environ., 29, 1441–1457.

- Lin, C.-J., and S. O. Pehkonen (1998), *Two-phase model of mercury chemistry in the atmosphere*, Atmos. Environ., 32, 2543–2558.
- Lin, C.-J., and S. O. Pehkonen (1999), *The chemistry of atmospheric mercury: A review*, Atmos. Environ., 33, 2067–2079.
- Liu, H., D. J. Jacob, I. Bey, and R. M. Yantosca (2001), *Constraints from ^{210}Pb and ^{7}Be on wet deposition and transport in a global three-dimensional chemical tracer model driven by assimilated meteorological fields*, J. Geophys. Res., 106, 12,109–12,128.
- Poissant, L., A. Amyot, M. Pilote, and D. R. S. Lean (2000), *Mercury water-air exchange over the Upper St. Lawrence River and Lake Ontario*, Environ. Sci. Technol., 34, 3069– 3078.
- Clever, H. L., S. A. Johnson, and M. E. Derrick, *The solubility of mercury and some sparingly soluble mercury salts in water and aqueous electrolyte solution*, d. Phys. Chem. Ref Data, 14, 631-680, 1985
- Xu, X., Yang, X., Miller, D. R., Helble, J. J. and Carley, R. J., 1999: *Formulation of bi-directional atmosphere surface exchanges of elemental mercury*. Atmos. Environ., **33**, 4345-4355.
- Poissant, L. and Casimir, A. (1998) *Water-air and soil-air exchange rate of total gaseous mercury measured at background sites*. Atmospheric Environment **32**, 883–893.
- Y Zhang, Y Tian, Y Knyazikhin, J Martonchik, D Diner, M Leroy and R.B Myneni, *Prototyping of MODIS LAI and FPAR algorithm with POLDER data over Africa,* IEEE Trans. Geosci. Remote Sens., 38 (2000), pp. 2402–2418
- M.M. Lynam, G.J. Keeler, *Source–receptor relationships for mercury in Urban Detroit, Michigan* Atmospheric Environment, 39 (2006), pp. 3144–3155
- Lyatt Jaegle, *Atmospheric Long-Range Transport and Deposition of Mercury to Alaska*-A report to the Alaska Department of Environmental Conservation, May 10, 2010